BRANDFORS
K 2016:4/2

Validation of a one-zone room fire model with well-defined experiments

Alexandra Byström, Johan Sjöström, Johan Andersson, Ulf Wickström

Brandforsk

BRANDFORSK 2016:4

Abstract

This report describes and validates a new simple calculation method for computing compartment fire temperature where flashover is reached. Comparisons are done with a series of experiments (Sjöström, et al., 2016).

Fire engineering design of structures and structural elements is in most cases made with procedures including a classification system and associated standard tests like ISO 834, EN 1363-1 or ASTM E-119 with defined time-temperature fire exposures. In these tests, fully developed enclosure fires are simulated in fire resistance furnaces with a prescribed duration. Other design fires (like the Eurocode parametric fire curves) are obtained by making a heat and mass balance analysis of fully developed compartment fires. A number of significant simplifications and assumptions are then done to limit the number of input parameters and facilitate the calculations. These are

- The fire compartment is ventilated by natural convection at a constant rate in terms of mass of air per unit time independent of temperature and time.
- The combustion rate is ventilation controlled, i.e. proportional to the ventilation rate.
- The gas temperature is uniform in the fire compartment.
- The fire duration is proportional to the amount of energy in the combustibles in the compartment, i.e. the fuel load.
- The energy of the fuel is released entirely inside the compartment.

The temperature development as a function of time may according to the new method in some idealized cases be calculated by a simple analytical closed form expression. With numerical analyses using ordinary finite elements codes for temperature calculations, this new way of modelling may be applied to surrounding structures of various compositions. Thus structures consisting of materials with properties varying with temperature and structures consisting of several layers may be analyzed (Byström, 2013; Byström, et al., 2016).

The model is based on an analysis of the energy and mass balance of a fully developed (ventilation controlled) compartment fire assuming a uniform temperature distribution. It is demonstrated in this report that the model can be used to predict fire temperatures in compartments with semi-infinite boundaries as well as with boundaries of insulated or uninsulated steel sheets where so called lumped heat capacity can be assumed. Comparisons are made with a series of experiments in compartments of light weight concrete, and insulated and non-insulated single sheet steel structures. A general finite element code has been used to calculate the temperature in the surrounding structures. According to the model the calculated surface temperatures of the surrounding structure yield the fire temperature depending on heat transfer conditions which in turn depend on ventilation conditions of the

compartment. By using a numerical tool like a finite element code it is possible to analyse fire compartment surrounding structures of various kinds and combinations of materials.

Two new characteristic compartment fire temperatures have been introduced in this paper, the *ultimate compartment fire temperature,* which is the temperature reached when heat losses to surrounding structures as well radiation out through openings can be neglected, and the *maximum compartment fire temperature*, which is the temperature when radiation out through openings is considered but not the losses to surrounding structures.

The experiments referred to were accurately defined and surveyed. In all the tests a propane diffusion gas burner was used as the only fire source. Temperatures were measured with thermocouples and plate thermometers at several positions, and oxygen concentrations were measured in the fire compartments only opening. In some tests the heat release rate as well as the CO_2 and CO concentrations were measured as well (Sjöström, et al., 2016).

The project is a collaboration between SP Fire Research and Luleå Technical University. It is fully financed by Brandforsk, the Swedish Fire Research Board.

Contents

Abstract 1

Preface 4

1. Introduction 5

2. Theoretical background 7

2.1 Heat balance of fully developed compartment fire 7

2.2 One-zone fire model, flashed over fires 7

Ultimate fire temperature, T_{ult} 9

Maximum fire temperature, T_{max} 10

Fire temperature in the flashed over compartment, T_f 10

3. Solution of the fire compartment temperature 15

3.1 Semi-infinite thick compartment boundary 15

3.2 Thin compartment boundaries 17

3.3 Numerical solution 18

4. Experimental setup 19

5. FE-modeling 23

6. Results and discussions 26

7. Conclusions 30

Bibliography 31

Appendix A - Thermal action according to Eurocode (EN 1991-1-2) 34

Appendix B – Simulation results: temperature calculated by FDS vs measured temperature 35

A series – LWC –Test A5 - 1000 kW. 37

C series – steel un-insulated –Test C2 - 1000 kW 40

Appendix C – Results from numerical simulation 43

Case A – Lightweight concrete compartment boundaries 43

Case B – steel structure insulated on the inside 46

Case C – Un-insulated steel compartment boundaries 48

Case D – steel structure insulated on the outside 49

Preface

This project was funded by the Swedish Fire Research Board (BRANDFORSK) which is greatly acknowledged.

1. Introduction

Several researchers have studied compartment fires. One of the first was carried out in Japan by Kawagoe (Kawagoe, 1958). Hurley (Hurley, 2005) compared in his work the temperature and burning rate predictions of several existing methods (Wickström, 1985; Lie, 2002; Magnusson & Thelandersson, 1970; Harmathy, 1972; Harmathy, 1972; Babrauskas, 1996; Ma & Mäkeläinen, 2000). All these methods have been evaluated by comparisons with fully developed post-flashover compartment fires conducted by several laboratories in the so called CIB experiments (Thomas & Heselden, 1972). These experiments were conducted in enclosures of reduced size and most of the test room models were constructed out of 10 mm thick asbestos millboard. Hurley's conclusion was that most of these models overestimate the fire temperature. A similar analysis has been done by Hunt and Cutonilli (Hunt & Cutonilli, 2010). In their work they compared 23 different empirical methods (some of them have been mentioned above) with the CIB experiments.

Magnusson and Thelandersson calculated in their work (Magnusson & Thelandersson, 1970) the gas temperature-time curves for compartments. Their models are based on the analysis of several experimental data, which have been analyzed with computer software. The model input data consists of fire load density, geometry of ventilations and thermal characteristics of the compartment enclosure (floor, walls and ceiling). Their model is usually known as the Swedish opening factor method. Magnusson and Thelandersson presented results (Magnusson & Thelandersson, 1974) in form of gas temperature-time curves of a complete process of fire for a range of opening factors and fuel loads, see Figure 1.

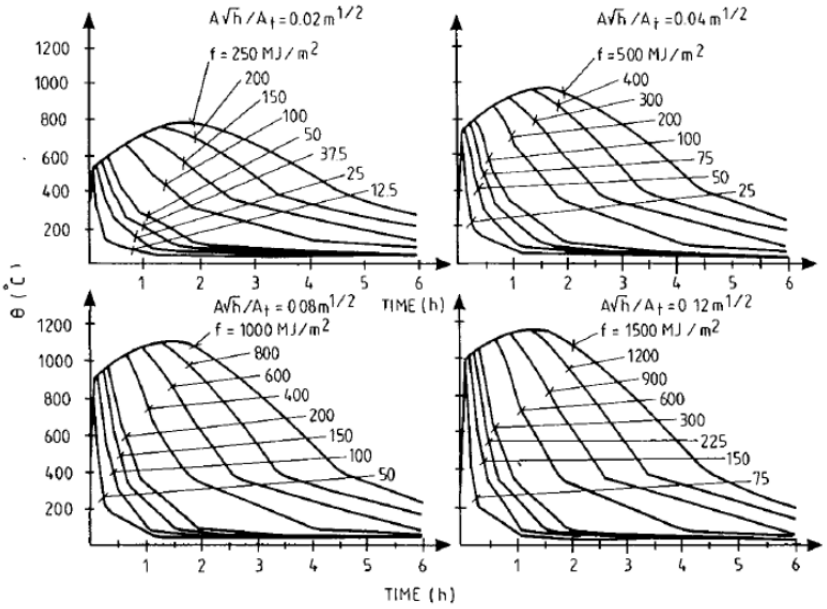

Figure 1. Temperature –time dependence of a fully developed fire for various fire load densities and opening factors (adapted from (Pettersson, et al., 1976))

Based on the work of Magnusson and Thelandersson (Magnusson & Thelandersson, 1970), Wickström (Wickström, 1985) proposed a modified way of expressing fully developed design fires based on the standard ISO 834 curve. This has later been adapted by the EN 1991-1-2.

Modelling and simulating the effect of fires in different geometries is a central part of fire safety engineering and fire risk assessments of structures. Many analytical models exist such as one- or two-zone models (Jones, 1983), closed-form hand calculations (Mowrer, 1992). There are simple numerical tools, e.g. BRANZFIRE (Wade, 2008) and more sophisticated fluid dynamics codes such as the Fire Dynamics Simulator, FDS, (McGrattan, et al., 1998).

This study aims at producing data for verification of models which take into account the thermal behavior of the enclosure materials. Even non-linear effects due to latent heat and radiation boundary conditions may then be considered which has not been possible with existing models. The report is based on the series of experiments performed using a gas burner with a known heat release rate and is summarized in (Sjöström, et al., 2016). For others to use, all the data can be downloaded in spreadsheet format or as diagrams (Sjöström & Wickström, 2015).

2. Theoretical background

This model is inspired by the Work of Magnusson and Thelandersson (Magnusson & Thelandersson, 1970). The thermal properties of the compartment boundaries will have a profound influence on the fire temperature development. The temperature development as a function of time may in some idealized cases be calculated by a simple analytical closed form expression (Wickström & Byström, 2014). With numerical analyses using ordinary finite elements codes for temperature calculations this new way of modelling may be applied to surrounding structures of various compositions. Thus structures consisting of several layers (even including voids) as well as materials with properties varying with temperature may be considered (Byström, 2013).

2.1 Heat balance of fully developed compartment fire

The heat balance of any compartment fire can be written as:

$$\left(\text{Heat release rate by combustion}\right) = \sum\left(\text{Heat loss rate }\right) \qquad (1)$$

Thus the heat balance for a fully developed fire compartment as shown in Figure 2 may be written:

$$\dot{q}_c = \dot{q}_l + \dot{q}_w + \dot{q}_r \qquad (2)$$

where $\dot{q}_c$ is the heat release rate in the compartment by combustion of fuel, $\dot{q}_l$ the heat loss rate due to the flow of hot gases out of the compartment openings, $\dot{q}_w$ the losses to the compartment boundaries and $\dot{q}_r$ is the heat radiation out through the openings. Other components of the heat balance equation are in general insignificant and not included in a simple analysis such as this.

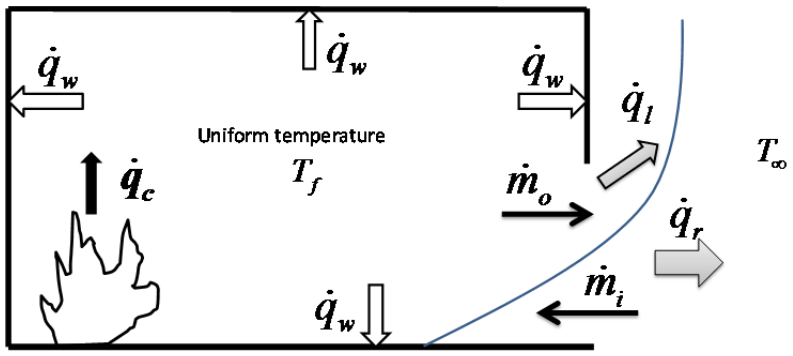

Figure 2: Heat balance for the post-flashover compartment fire.

2.2 One-zone fire model, flashed over fires

The new simple calculation method for compartment temperatures has been discussed early in (Wickström & Byström, 2014; Sundström & Gustavsson, 2012). This model is applicable to post-flashover compartment fires, i.e. for ventilation controlled fires (a uniform gas

temperature is assumed) and even can be used for pre-flashover fire in enclosures where the heat capacity is lumped into the core of the surrounding structure (Evegren & Wickström, 2015).

It is based on energy and mass balance of the fire compartment as indicated in Figure 2 applying conservation principles, which has been discussed in an earlier publication (Wickström & Byström, 2014).

According to the conservation principles the mass flow rate of the gases out of the compartment $\dot{m}_o$ must be equal to the mass flow rate of the fresh air entering the compartment $\dot{m}_i$ (here the mass of the gases generated by the fuel is neglected):

$$\dot{m}_i = \dot{m}_o = \dot{m}_a \tag{3}$$

For vertical openings, the flow rate can be described as being approximately proportional to the opening area times the square root of its height:

$$\dot{m}_a \approx \alpha_1 A_o \sqrt{H_o} \tag{4}$$

where the proportionality constant $\alpha_1 = 0.5$ is a flow constant, A_o and H_o are the area and height of the openings of the compartment, respectively.

The combustion rate $\dot{q}_c$ inside the ventilation controlled compartment can be written as:

$$\dot{q}_c = \chi \alpha_2 \dot{m}_a \tag{5}$$

where χ is the combustion efficiency and α_2 a constant describing the combustion energy developed per unit mass of air (Wickström & Byström, 2014). The combustion efficiency χ is assumed to be in the range of 40 % - 70 % (Drysdale, 1998).

The convection loss term is proportional to the mass flow times the fire temperature increase, i.e:

$$\dot{q}_l = c_p \dot{m}_a (T_f - T_i) \tag{6}$$

where c_p is the specific heat capacity of the combustion gases (usually assumed equal to that of air), T_f and T_i are the fire and the initial (and ambient) temperatures, respectively.

The wall loss term $\dot{q}_w$ is proportional to the total surrounding area of the enclosure A_{tot}:

$$\dot{q}_w = A_{tot} \dot{q}''_w \tag{7}$$

where $\dot{q}''_w$ is the heat flux rate to the enclosure surfaces. This term constitutes the inertia of the system (Wickström & Byström, 2014).

Finally the heat radiating out through the openings may be calculated as:

$$\dot{q}_r = A_o \sigma (T_f^4 - T_\infty^4) \tag{8}$$

where T_∞ is the ambient temperature.

By inserting Eq. (5), Eq. (6), Eq. (7) and Eq. (8) into Eq. (1) we get:

$$\chi \alpha_2 \dot{m}_a = c_p \dot{m}_a (T_f - T_i) + A_{tot} \dot{q}''_w + A_o \sigma (T_f^4 - T_\infty^4) \tag{9}$$

Then by replacing $\dot{m}_a$ according to Eq. (4) and rearranging, we get

$$\dot{q}''_w = c_p \alpha_1 O \left(\frac{\chi \alpha_2}{c_p} - \theta_f \right) + \frac{A_o}{A_{tot}} \sigma (T_\infty^4 - T_f^4) \tag{10}$$

where O is the so called *opening factor* defined as

$$O = \frac{A_o \sqrt{H_o}}{A_{tot}} \tag{11}$$

and θ_f the fire temperature increase defined as:

$$\theta_f = T_f - T_i \tag{12}$$

Ultimate fire temperature, T_{ult}

Assume a closed compartment without radiation losses through the openings and perfectly insulated boundaries, i.e. no heat loss through the boundaries. Then by inserting Eq. (5), Eq. (6), $\dot{q}_w = 0$ and $\dot{q}_r = 0$ in the heat balance equation, Eq. (2), we get:

$$\chi \alpha_2 \dot{m}_a = c_p \dot{m}_a (T_f - T_i) + 0 + 0 \tag{13}$$

In this case a very high temperature can be reached, the so called **ultimate compartment fire temperature rise**, θ_{ult} (Wickström & Byström, 2014; Wickström, 2016), obtained from Eq. (13):

$$\theta_{ult} = T_f - T_i = \frac{\chi \alpha_2}{c_p} \tag{14}$$

The ultimate temperature fire temperature, $T_{ult} = \theta_{ult} + T_i$, will generally not be obtained in reality as fire compartments have openings. Exceptions are furnaces and tunnels where very high temperatures may develop. It is introduced here to facilitate the derivation and explanation of the fire temperature development model.

The ultimate temperature is directly proportional to the combustion efficiency χ. In reality, it is hard to estimate the combustion efficiency in a real fire. That is why some assumptions should be made. For the numerical solution when the heat loss through the openings is taken

into numerical analysis, a higher value of combustion efficiency of 60 % is assumed (Byström, 2013).

Maximum fire temperature, T_{max}

Let us now assume that the compartment has perfectly insulated boundaries, i.e. no heat loss through the boundary. By inserting Eq. (5), Eq. (6), Eq. (8) and $\dot{q}_w = 0$ in the heat balance equation, Eq. (2) we get:

$$\chi\alpha_2\dot{m}_a = c_p\dot{m}_a(T_f - T_i) + 0 + A_o\sigma(T_f^4 - T_\infty^4) \tag{15}$$

Solving Eq. (10) with respect to T_f (equation of the fourth grade) will give the value of the maximum temperature of compartment fire T_{max} which can be reached when the losses to the walls are neglected .

Fire temperature in the flashed over compartment, T_f

By inserting Eq. (14) into Eq. (10) the equation for the calculation fire temperature can be expressed as:

$$\dot{q}''_w = c_p\alpha_1 O\left(\theta_{ult} - \theta_f\right) + \frac{A_o}{A_{tot}}\sigma(T_\infty^4 - T_f^4) \tag{16}$$

Eq. (16) is analogous to the heat transfer equation by convection and radiation between a gas and a solid surface. This may be seen as an analogous electrical model, see Figure 3. Eq. (16) can then be written as:

$$\dot{q}''_w = \frac{1}{R_{f.c}}\left(\theta_{ult} - \theta_f\right) + \frac{1}{R_{f.r}}(T_\infty - T_f) \tag{17}$$

where the two heat transfer resistances can be identified as:

- Fire compartment thermal resistance due to convective heat transfer

$$R_{f.c} = \frac{1}{h_{f.c}} = \frac{1}{c_p\alpha_1 O} \tag{18}$$

- Fire compartment thermal resistance due to radiation heat transfer

$$R_{f.r} = \frac{1}{h_{f.r}} = \frac{1}{\hat{\varepsilon}\sigma\left(T_\infty^2 + T_f^2\right)\left(T_\infty + T_f\right)} \tag{19}$$

Where ration A_o/A_{tot} can be associated by analogy with an emissivity, i.e. $\hat{\varepsilon} \equiv A_o/A_{tot}$

As we can see Eq. (17) is analogous to the heat transfer equation by convection and radiation between the gas and solid surface. So the thermal conditions may be seen as the analogous electrical model, Figure 3:

Therefore the heat transfer between fire temperature and the surface according to (Wickström, 2016) and Figure 3 and Figure 4 can be described as:

$$\dot{q}''_w = \frac{1}{R_{i.tot}}(T_f - T_s) = \frac{1}{R_{i.c}}\left(T_f - T_s\right) + \frac{1}{R_{i.r}}(T_f - T_s) \tag{20}$$

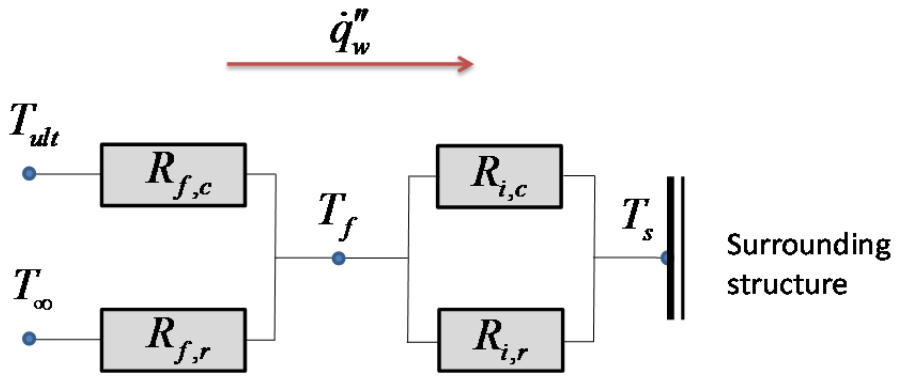

Figure 3. Electric circuit analogy model of a fire compartment boundary according to the new model.

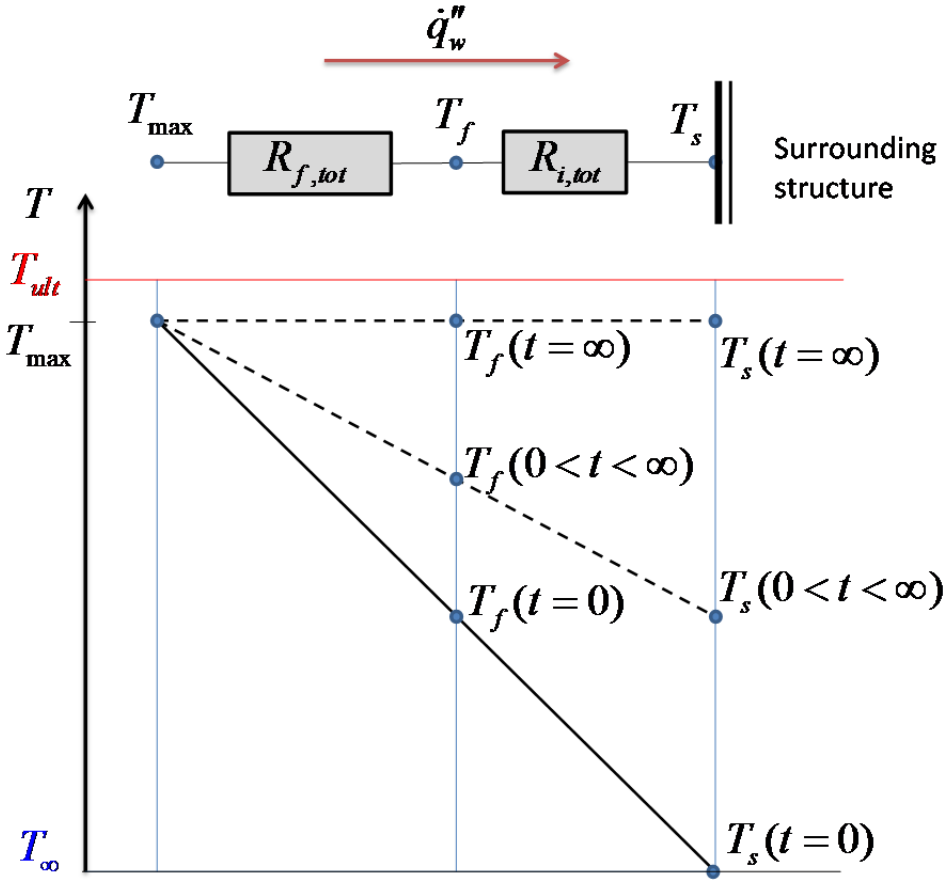

Figure 4. Electrical analogy of the fire model for any structure. The indication of the temperature initially (t=0), after some time (0<t<∞) and after a very long time (t=∞).

where the total thermal resistance $R_{i.tot} = \dfrac{1}{1/R_{i.r} + 1/R_{i.c}}$ and the thermal resistance due to convective heat transfer between fire temperature and surface temperature is:

$$R_{i.c} = \frac{1}{h_{i.c}} \tag{21}$$

The convective heat transfer coefficient, $h_{i.c}$, for the walls in the enclosure can be assumed to be in the range 25-50 W/m^{2}K on exposed to fire sides (EN 1991-1-2).

Moreover, the fire compartment thermal resistance due to radiation heat transfer is:

$$R_{i.r} = \frac{1}{h_{i.r}} = \frac{1}{\varepsilon_s \sigma \left(T_f^2 + T_s^2\right)\left(T_f + T_s\right)} \tag{22}$$

where ε_s is emissivty of the exposed surfaces.

The two temperatures T_{ult} and T_∞ may be reduced to one resultant temperature $T_{\max}$ which a weighted mean value of the two, see Eq. (15). Compare with theory behind the adiabatic surface temperature, see (Wickström, 2016). Then the electric circuit of Figure 3 can be can reduced that of Figure 4.

As it has been described above $T_{\max}$ is the maximum temperature a compartment fire can reach is when the losses to the walls vanish. It can be calculated according to Eq. (15).

As there is no thermal heat capacity involved the heat flux may also be written as

$$\dot{q}''_w = \frac{T_{\max} - T_s}{R_{f.tot} + R_{i.tot}} \tag{23}$$

where

$$T_{\max} = \frac{R_{f.c} T_\infty + R_{f.r} T_{ult}}{R_{f.c} + R_{i.r}} \tag{24}$$

and

$$R_{f.tot} = \frac{1}{1/R_{f.r} + 1/R_{f.c}} \tag{25}$$

Fire temperature in the flashed over compartment – assumption for FE modeling with Tasef, T_f

To be able to validate experiments with the model, see Eq. (16), by using FE code TASEF some assumption and simplifications has been made.

Eq. (20) can be also written as::

$$\dot{q}''_w = \frac{1}{R_{i.tot}} (\theta_f - \theta_s) \tag{26}$$

so that the fire temperature θ_f can be expressed as:

$$\theta_f = \dot{q}''_w R_{i.tot} + \theta_s \tag{27}$$

Inserting Eq. (27) into Eq. (10) gives:

$$\dot{q}''_w = \frac{1}{R_{f.c}}\left(\theta_{ult} - \dot{q}''_w R_{i.tot} - \theta_s\right) + \frac{A_o}{A_{tot}}\sigma(T_\infty^4 - T_f^4) \tag{28}$$

Rearranging Eq. (28) gives:

$$\dot{q}''_w = \frac{1}{R_{f.c} + R_{i.tot}}\left(\theta_{ult} - \theta_s\right) + \frac{A_o}{A_{tot}}\frac{R_{f.c}}{R_{f.c} + R_{i.tot}}\sigma(T_\infty^4 - T_f^4) \tag{29}$$

For numerical analysis Eq. (29) can be interpreted as a boundary condition for a one-dimensional structure exposed to radiation and convection as indicated by Figure 4. For the model of the heat transferred by radiation the assumption $T_s = T_f$ has been made. Then the surface temperature can be calculated by FE modelling (Tasef has been used), and the fire temperature θ_f can be obtained as a weighted average between θ_{max} and the calculated surface temperature θ_s as:

$$\theta_f = \frac{\theta_s R_{f.tot} + \theta_{\max} R_{i.tot}}{R_{f.tot} + R_{i.tot}} \tag{30}$$

where $R_{f.tot}$ is the artificial thermal resistance between the θ_{max} and the fire temperature, and $R_{i,tot}$ is the thermal resistance between the fire temperature and the surface, and where

$$R_{f.tot} = \frac{1}{1/R_{f.c} + 1/R_{f.r}} \tag{31}$$

Based on the work described earlier (Byström, 2013; Wickström & Byström, 2014) for the numerical analysis, Eq. (29) can be interpreted as a boundary condition for a structure exposed to radiation and convection where the heat transfer is expressed as:

$$\dot{q}''_w = h_{FE}(T_{ult} - T_s) + \varepsilon_{FE}\sigma(T_\infty^4 - T_f^4) \tag{32}$$

This theory will be used for the numerical analysis with following parameters, Table 1. All parameters which have been used in the model are collected in Table 2.

Table 1. Analogue parameters for the FE-modelling with Tasef.

Emissivity	*Convection heat transfer coefficient*	*Ultimate fire temperature*
$\varepsilon_{FE} = \frac{A_o}{A_{tot}}\left(1+\frac{R_{i.tot}}{R_{f.c}}\right)^{-1}$	$h_{FE}\frac{1}{R_{f.c}+R_{i.tot}} = \left(\frac{1}{c_p\alpha_1 O}+\frac{1}{h_{i.tot}}\right)^{-1}$	$\theta_{ult}+T_i = \frac{\chi\alpha_2}{c_p}+T_i$

Table 2 Values of physical parameters and parameter groups.

Parameter	*Notation, value, units*
Combustion efficiency: *a) For analytical solution,* (Wickström & Byström, 2014; Wickström, 2016) *b) For FE analysis* (Byström, 2013; Byström, et al., 2016)	$\chi = 50\%$ $\chi = 60\%$
Proportionality constant (called a *flow constant)*	$\alpha_1 = 0.5\,{kg}/{m^{2.5}s}$
Combustion yield coefficient - Constant describing the combustion energy developed per unit mass of air	$\alpha_2 = 3.01\cdot10^6\,{Ws}/{kg}$
Specific heat capacity of the combustion gases (usually assumed equal to that of air)	$c_p = 1150\,{Ws}/{kg\cdot K}$
Fire temperature:	T_f
Ambient temperature	$T_\infty = 20^oC$
Initial temperature	$T_i = 20^oC$
Ultimate temperature, Eq.(14)	$\chi = 60\% \rightarrow T_{ult} = 1592^oC$
Fire temperature increase	$\theta_f = T_f - T_i$
Heat flux rate to the enclosure surfaces	$\dot{q}''_w$

3. Solution of the fire compartment temperature

For some idealized cases of compartment boundaries, an analytical solution can be applied :

- Compartments with semi-infinite thermal thick boundaries (Sundström & Gustavsson, 2012; Wickström & Byström, 2014; Wickström, 2016)
- Compartments with boundaries being thermally thin, where the heat capacity is concentrated in a core (so called lumped heat capacity) ((Wickström, 2016)

Limitation/assumption of the analytical solution:

- All materials properties must be remain constant
- Heat transfer coefficients between fire gases and surrounding surfaces must remain constant
- No radiation losses through the openings, $\dot{q}_r = 0$
- The heat radiated directly out the openings, $\dot{q}_r$, is neglected or is directly proportional to the difference between the fire temperature T_f and the ambient temperature T_∞, i.e. $h_{f.tot}$ and its reciprocal $R_{f.tot}$ are constant.
- The heat transfer by radiation and convection to the surrounding boundaries is assumed proportional to the difference between the fire temperature T_f and boundary surface temperatures T_s, i.e. $h_{i.tot}$ and its reciprocal $R_{i.tot}$ are constant.

3.1 Semi-infinite thick compartment boundary

Fire compartment boundaries are in most cases assumed thermally thick. The heat transferred to the surfaces are then stored in the surrounding structures and the effects of heat lost on the outside of the structure is neglected.

As discussed earlier, see Figure 4, the boundary condition may be expressed by two thermal boundary resistances in series which can be added up and the complete thermal model becomes as described in Figure 5.

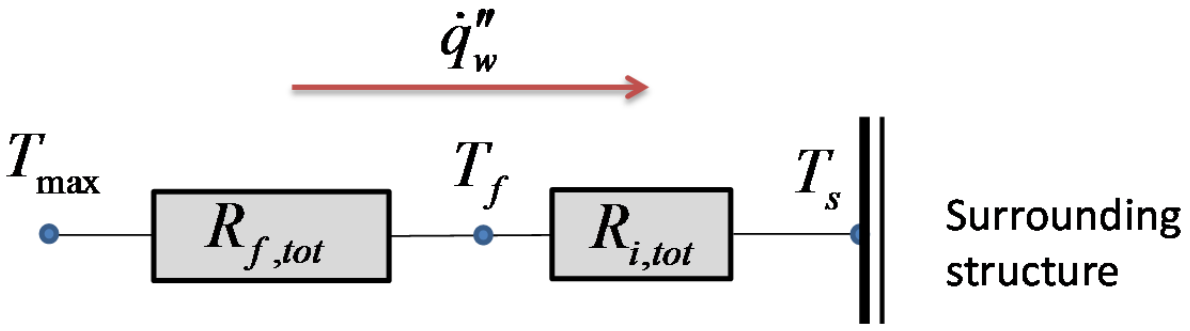

Figure 5 Electric circuit analogy model of a fire compartment with infinitely thick walls.

This is a third kind of boundary condition. This third kind of boundary condition (sometimes called a natural boundary condition) means that the heat flux to the boundary depends on specified surrounding temperatures and the surface temperature. In its simplest form the heat flux is proportional to the difference between the surrounding gas temperature and the surface temperature. The proportionality constant is denoted the heat transfer coefficient and can be in general expressed as:

$$h\left(T_g - T_x\right) = -k\left.\frac{\partial T}{\partial x}\right|_{x=0} \tag{33}$$

In case of compartment fire, in order to compute the surface temperature we generally need to use numerical temperature calculation methods such as finite element methods. The fire temperature is calculated as the weighted mean temperature of $T_{\max}$ and T_s according to Eq. 24.

The surface temperature (x=0) can be found by solving Eq. (33) which is described more in detail by (Wickström, 2016) as:

$$\frac{T_s - T_i}{T_g - T} = 1 - e^{\left(\frac{t}{\tau}\right)} erfc\sqrt{\frac{t}{\tau}} \tag{34}$$

where in general cases the time constant τ for the semi-infinite case is defined as, according to (Wickström, 2016):

$$\tau = \frac{k\rho c}{h^2} \tag{35}$$

In most cases considered in the literature, fire compartment boundaries are assumed thermally thick. Based on this assumption and in analogy with the general solution of the surface temperature of a semi-infinite body, see for example (Holman, 2010), the fire temperature development in a fire compartment surrounded by semi-infinite structures may be written as,

$$\theta_s = \theta_{\max}\left[1 - e^{\left(\frac{t}{\tau_f}\right)} erfc\sqrt{\frac{t}{\tau_f}}\right] \tag{36}$$

where the parameter τ_f may be identified as a *fire compartment time constant* for infinitely thick compartment boundaries in analogy with Eq. 35:

$$\tau_f = \frac{k\rho c}{\left(\frac{1}{R_{f.tot} + R_{i.tot}}\right)^2} = k\rho c\left(R_{f.tot} + R_{i.tot}\right)^2 \tag{37}$$

where $R_{f.tot}$, Eq. (25), is the thermal resistance between the $\theta_{\max}$ and the fire temperature and $R_{i.tot}$, the thermal resistance between the fire temperature and the surface. Constant values of the resistances must be assumed to obtain an analytical solution. Then a constant value must be assumed to calculate the resistances referring to radiation. Too high assumed T_f values will yield overestimated heat losses by radiation out through the openings and therefore underestimated fire temperatures, and vice versa.

Combining Eq. (30) and Eq. (36) and rearranging it with respect to θ_f becomes:

$$\theta_f = \frac{\theta_{\max}}{1+\frac{R_{i.tot}}{R_{f.tot}}}\left(\left[1-e^{\left(\frac{t}{\tau_f}\right)}erfc\sqrt{\frac{t}{\tau_f}}\right]+\frac{R_{i.tot}}{R_{f.tot}}\right) \tag{38}$$

In reality the heat transfer resistance between the fire gases and the surfaces of the compartment boundaries depends on temperature increase and not constant. And the radiation heat loss through the compartment openings must be considered. This can be done numerically by using FE modeling.

A detailed procedure of how to reach the analytical solution with some examples for semi-infinite structure boundaries can be found in the work presented earlier (Wickström & Byström, 2014; Wickström, 2016)

3.2 Thin compartment boundaries

Analytical solutions of fire temperatures may also be obtained when the fire compartment is assumed surrounded by structures consisting of a metal core where the all the heat capacity is concentrated, so called lumped heat. Thus the capacity per unit area C_{core} may be approximated as lumped into the core, see Figure 6) as discussed before (Wickström & Byström, 2014). In addition, the heat capacity of any insulating material is either neglected or assumed included in the heat capacity of the core.

The analytical solution is possible only in the case when the heat lost by radiation through the opening is neglected as it mentioned above. In reality, the radiation heat loss through the compartment openings must be considered, in particular when high fire temperatures are anticipated. In such cases numerical solution techniques are required.

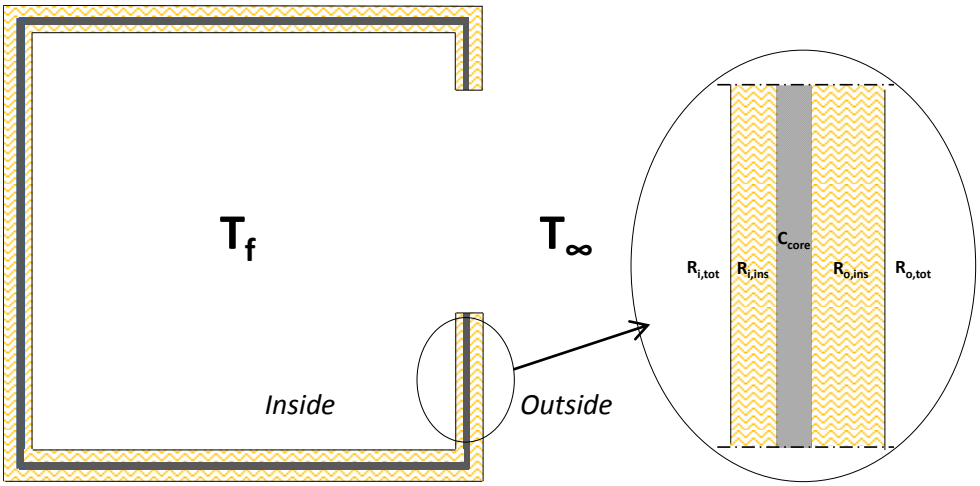

Figure 6 A fire compartment surrounded by a structure with its heat capacity C_core assumed concentrated/lumped to a metal core. Thermal resistances of insulation materials R_i and R_o are assumed on the fire inside and outside, respectively.

A detailed procedure of how to find an analytical solution can be found in the work presented by Sundström and Gustavsson (Sundström & Gustavsson, 2012; Wickström, 2016).

3.3 Numerical solution

The purpose of using finite element modelling is that we can include non-linear phenomena like the heat loss rate by radiation through vertical openings in the one dimensional heat transfer analysis as well as material properties varying with temperature. Since the radiation through vertical openings is having a combustion efficiency of 60 %, which will give a ultimate compartment fire temperature temperature of $T_{ult} = \theta_{ult} + 20 = 1592\,[°C]$ according to the theory above.

The use of numerical analysis also gives us the opportunity to predict fire compartment temperatures with different material layouts of the walls (Byström, 2013).

4. Experimental setup

The experiments were conducted at the SP Fire Research. For more data and information about the experimental setup and result see report (Sjöström, et al., 2016).

The inner structure was representing a small office in scale 3:4. The inner dimensions were 1800 mm by 2700 mm and a height of 1800 mm. Centrally on one of the short ends was a 600 mm by 1500 mm high doorway opening, see Figure 7. The materials and thicknesses of the walls were changed between the test series. The same materials were used in floor, ceiling and walls.

Figure 7 Left: inner dimensions of the enclosure. Right: test object of 100 mm lightweight concrete.

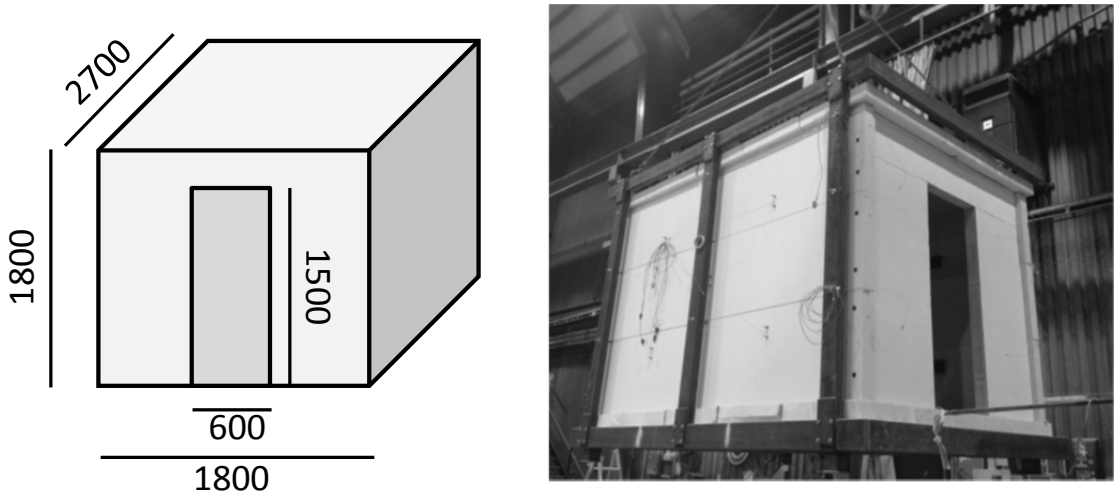

A diffusion propane burner (300 mm by 300 mm) was placed in the middle of the enclosure. The gas burner was filled to half its volume with gravel (~10-20 mm stones). Five different fire scenarios were conducted ((Sjöström, et al., 2016), see table 3

Table 3. Fire loads.

Fire load number	HRR (kW)	Placement of burner	Used in test series
1	1000	Central	A, B, C, D
2	500	Central	A, C
3	1000	Centre of back wall	A
4	250 + 20[kW/min]*t[min] Constant at 1250 kW after 50 min.	Central	A
5	200 + 60[kW/min]*t[min] Constant at 1250 kW after 17.5 min.	Central	C

Fire load number 1 has been chosen for validation. In this model the heat release rate was kept constant at 1000 kW and burner was centrally placed.

Five experiments have been selected and compared, for more detailed information about the experiments, see (Sjöström, et al., 2016):

Light weighted concrete (LWC) boundaries, see Figure 7**.** The first experiment **(Test A1)** was conducted in a compartment with the structures containing its original moisture. The density of the material was measured before testing to be around 760 kg/m^3, containing 39 % of moisture (dry basis by weight). The second experiment **(Test A5)** was conducted in the same compartment after a series of fire experiments. Thus it can be assumed that the concrete had dried out. More details for the original concrete as well as for the concrete after exposure in a furnace of 105 °C during 24 h are found in Table 4.

Insulated steel boundaries. Test series B **(Test B2)** was conducted in a 3 mm thick steel structure. The inner dimensions of the steel enclosure were as shown in Figure 7. However, the width/length/height of the inner surfaces in test series B were 100 mm smaller as the inside was covered with 50 mm stone wool boards, i.e. the inner dimensions were then 1700 by 2600 by 1700 mm with a door opening of 1450x600 mm^2. Test series D **(Test D2)** was conducted on the same steel structure as test series B but with the stone wool insulation on the outside. The stone wool had a nominal density of 200 kg/m^3 and a nominal room temperature conductivity of 0.04 W/mK.

Uninsulated steel boundaries. Test series C **(Test C2)** was conducted on the same steel structure as test series B but without any insulation.

Table 4. Nominal thermal material properties at room temperature

Material	Specific heat, (J/kgK)	Thermal conductivity at room temperature, (W/mK)	Density, (kg/m^3)
Light weight concrete, original	851 (±19)	0.330 (±0.009)	760
Light weight concrete, dried (after exposure in a furnace of 105 °C during 24 h)	835 (±16)	0.166 (±0.006)	-
Stone wool	-	0.04	200

Several thermocouple trees were installed to measure gas temperatures at various heights, for experiments Series A see Figure 8, otherwise see Figure 9. The walls and ceiling in the enclosure was instrumented by thick plate thermometers (PT) described in (Sjöström & Wickström, 2013) and previously used in many field experiments (Sjöström, et al., 2013; Sjöström & Anderson, 2013). The PTs are positioned a fourth of the distance from adjacent walls/floor/roof as well as in the center and are indicated as squares on all inner surfaces in Figure 8. An additional PT is positioned 1000 mm from the door opening at 600 above floor level. In total, more than 50 measuring devices were installed during each experiment. In this report only the read out from the Standard Plate Thermometers (PT) measurements have been selected, analysed and compared with calculated temperatures.

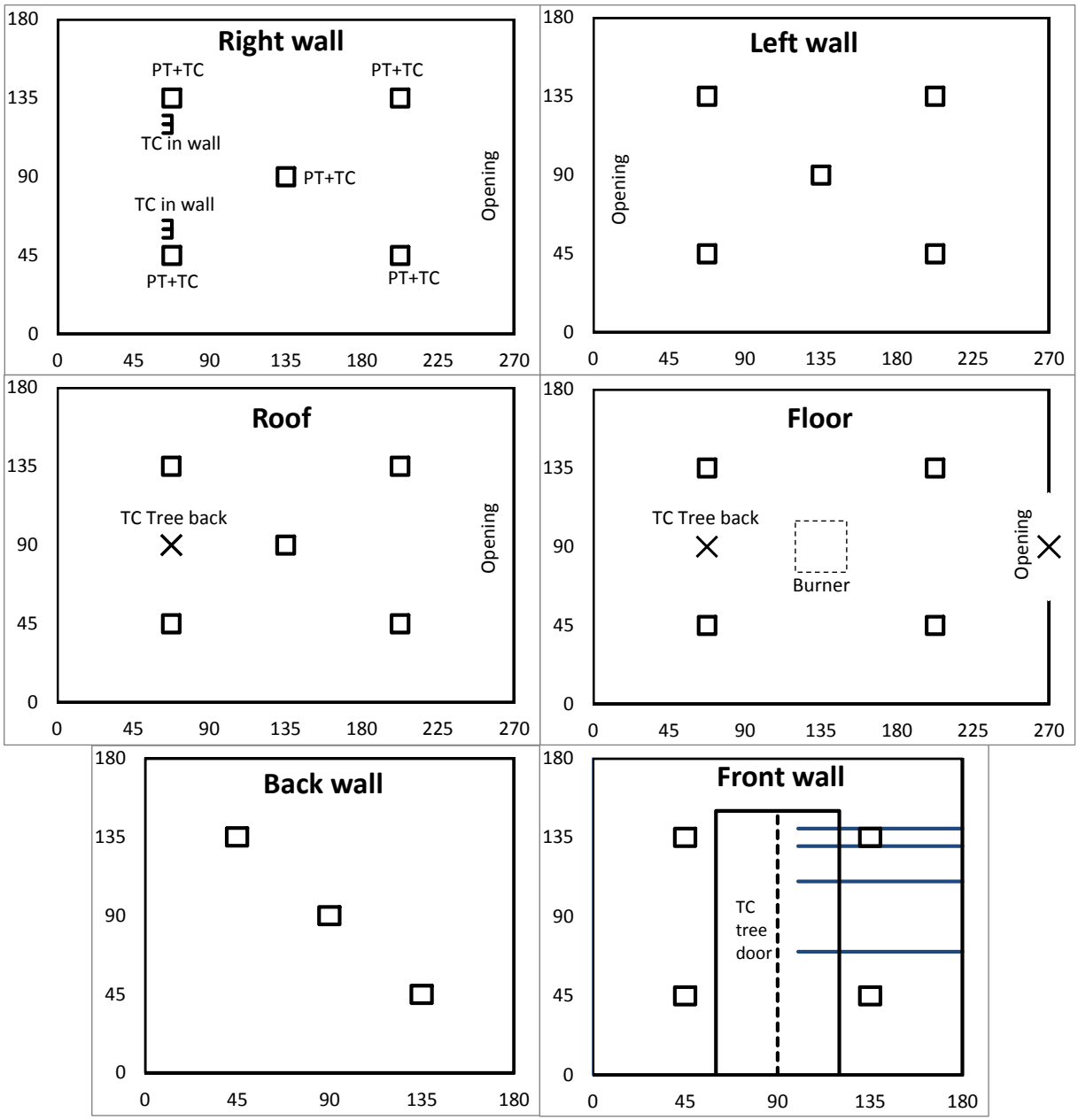

Figure 8 The instrumentation at the inside of the enclosure for test series A. The distances are in cm. All squares are PT only unless stated otherwise. The back TC tree spans from roof to floor and the door TC tree from top to bottom of the opening. O2 gas measurements are measured in the opening a distance 100, 200, 400 and 800 mm from the top of the opening.

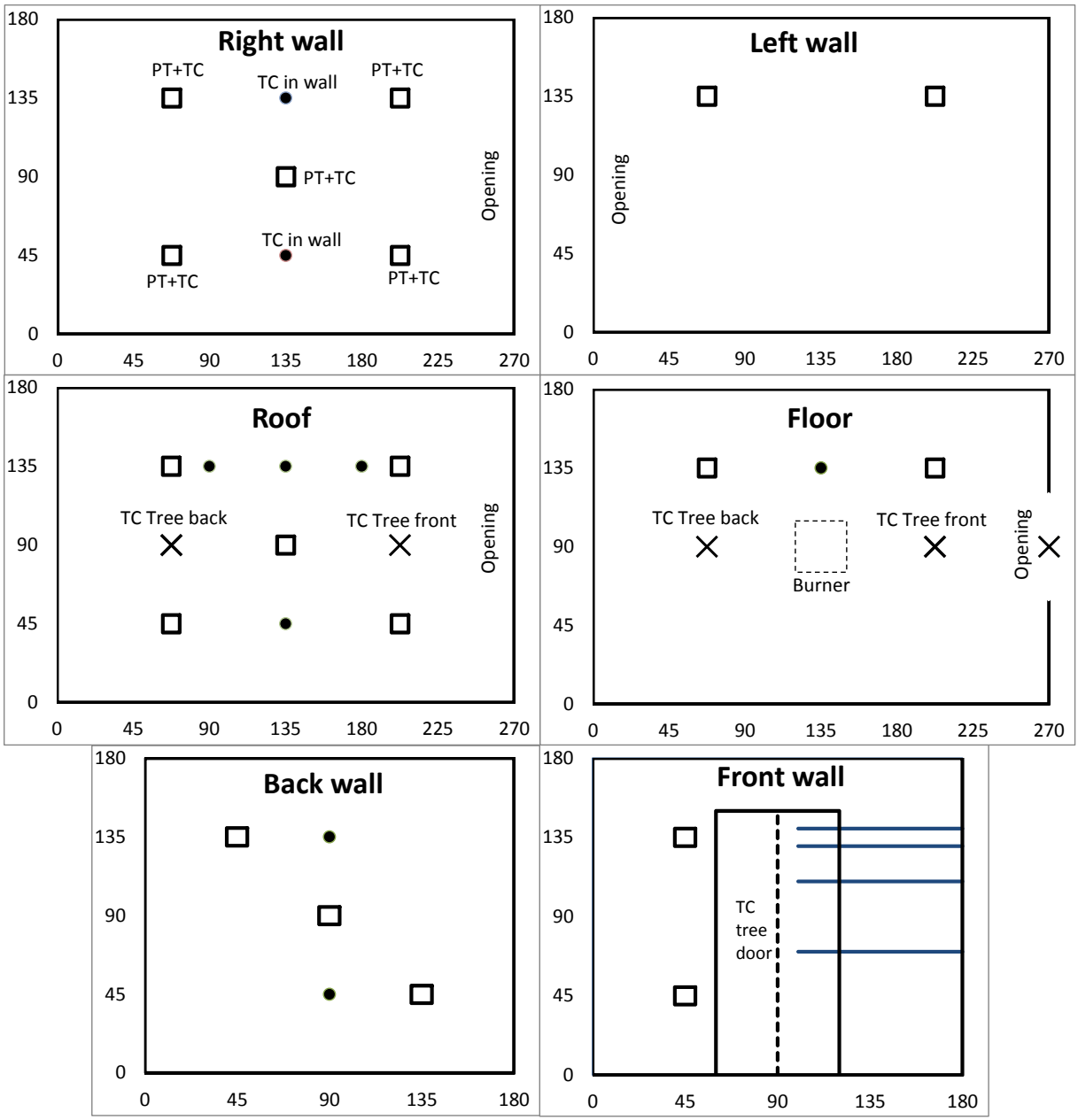

Figure 9 The instrumentation at the inside of the enclosure for test series C and D. The distances are in cm. All squares are PT only unless stated otherwise. All black points are steel temperature measurements. The tubes in the door opening measures CO, CO2 and O_2 gas concentrations at heights 100, 200 and 800 mm from the top of the door opening

5. FE-modeling

The purpose of using finite element modelling is that we can include non-linear phenomena like the heat loss rate by radiation through vertical openings in the one dimensional heat transfer analysis as well as material properties varying with temperature. It also opens for the possibility to predict fire compartment temperatures with different material combinations like e.g. gypsum stud walls.

Due to the same material on all surrounded structures a one-dimensional heat transfer analysis was considered. To calculate surface temperatures according to the theory described above, the finite element code TASEF (Wickström, 1979) was used. TASEF is capable of solving one- and two-dimensional, axisymmetric heat transfer problem.

Assumptions:

- A combustion efficiency of 60 % is assumed according to the theory above, so that the ultimate temperature was calculated to $T_{ult} = 1592^{o}C$ according to the Eq. (15), see also (Byström, 2013)
- The heat transfer resistance between the fire gases and the exposed surface is kept at a constant value due to limitations of the FE program. The assumed value is reasonable for the final stage but not for the first minutes of temperature increase, see more in **Appendix C**

- The heat transfer coefficient by convection on the unexposed side was assumed equal to 4 W/m^{2}K and the surface emissivity 0.9.
- The emissivities of the light weight concrete surfaces were assumed equal to 0.8 both on the exposed and the unexposed sides.

Material properties

The measured material properties, mentioned above, in Table 4 and (Sjöström, et al., 2016), have been applied in the FE-analysis. For the steel, Eurocode 4 properties were assumed and for the stone wool we assumed properties based on producer data available on the web and extrapolated for higher temperatures, see Figure 10.

Figure 10 Thermal conductivity of the stone wool used for the FE-modeling

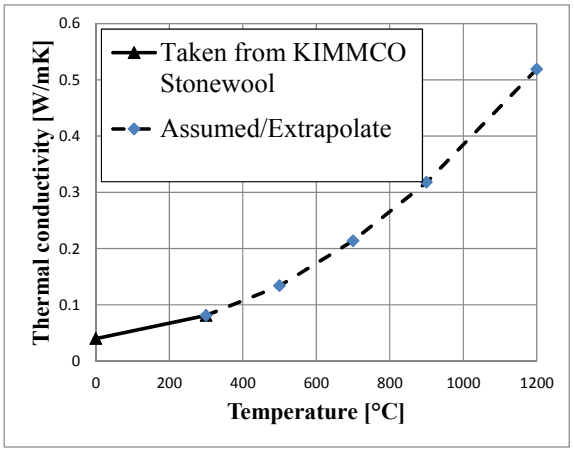

To apply the model described above some **boundary conditions** have been described as radiation and convection on exposed fire surface.

Heat transfer by radiation

Radiation will be a negative term her, due to radiation losses through the opening. The artificial emissivity of the exposed surface was calculated according to Table 1:

$$\varepsilon_{FE} = \frac{A_o}{A_{tot}} \frac{1}{\left(1 + \frac{R_{h.i}}{R_f}\right)} \tag{39}$$

All parameters for the FE modelling have been summarized in Table 5.

Since heat transfer by radiation on exposed to fire surface is actually radiation losses through the opening, as mentioned above, it can be expressed as:

$$\frac{A_o}{A_{tot}} \frac{R_f}{R_f + R_{h,i}} \sigma(T_\infty^4 - T_f^4) = \varepsilon_{FE} \sigma(T_\infty^4 - T_f^4) \tag{40}$$

where for this expression only, we can assume that the fire temperature and the surface temperature are equal, $T_f = T_s$, that is, we assume that the radiation losses through the opening actually comes from the surface temperature.

Heat transfer by convection

The convective heat transfer coefficient on the exposed surface is calculated according to theory above, see Table 1:

$$h_{FE} = \frac{1}{R_f + R_{h,i}} = \frac{1}{\frac{1}{c_p \alpha_1 O} + \frac{1}{h_i}} \tag{41}$$

All parameters for the FE modelling have been summarized in Table 5.

Since heat transfer by convection on exposed to fire surfaces depends on the ultimate fire temperature, as mentioned above, it can be expressed as:

$$\frac{1}{R_f + R_{h,i}}\left(\theta_{ult} - \theta_s\right) = h_{FE}\left(\theta_{ult} - (T_s - T_i)\right) = h_{FE}\left((\theta_{ult} + T_i) - T_s\right) \tag{425}$$

where the ultimate temperature, θ_{ult} (see Eq.(15)), depends only on the combustion yield α_2, combustion efficiency χ and the specific heat capacity of air c_p, but is independent of the air mass flow rate, of the fire compartment geometry and of the thermal properties of the compartment boundaries.

Table 5 Parameters used for FE analysis

Parameter	Value	Units
Parameters depending on compartment and openings dimensions		
Area of openings	$A_o = H_o \cdot B_0 = 1.5 \cdot 0.6 = 0.9$	m^2
Height of openings	$H_o = 1.5$	m
Total surrounding area of enclosure (excluding openings)	$A_{tot} = 25.02$ (case A, C and B) $A_{tot} = 22.56$ (case D)	m^2
Opening factor, Eq A.10	$O = \frac{A_o\sqrt{H_o}}{A_{tot}}$	$m^{1/2}$
Fire heat transfer resistance	$R_f = \frac{1}{c_p \alpha_1 O} = \frac{1}{1150 \cdot 0.5 \cdot 0.04} = \frac{1}{23}$	m^2K/W
Parameters, independent on compartment and openings dimensions		
Ambient temperature	$T_\infty = 20$	^oC
Ultimate compartment fire temperature	$\theta_{ult} = \frac{\chi\alpha_2}{c_p} = 1572$ for χ=60%	^oC or K
Initial temperature	$T_i = 20$	^oC
Total heat transfer thermal resistance at the fire exposed surface, assumed to be constant	Assumed $R_{h.i} = \frac{1}{h_i} = \frac{1}{h_{rad} + h_{conv}} = \frac{1}{4\varepsilon\sigma T_s^4}$	m^2K/W

6. Results and discussions

The results of the measured maximum and minimum temperatures during the experiments conducted in the enclosure with various boundaries are given Figure 11.

The mean temperature is calculated based on the average temperature to the fourth power (the radiative potential) from all readout of the PT measurements around the whole compartment, see Eq. (43). In test series A it was 25 PTs in total and for the rest of experiments 17. For more detailed information of the location of PT see report (Sjöström, et al., 2016)

$$T_{PT.mean} = \sqrt[4]{\frac{\sum\left(T_{PT.i}{}^{4} \cdot A_{PT.i}\right)}{A_{tot}}} \tag{43}$$

Fire temperatures numerically calculated by using the new model have been compared with experimentally measured temperatures. Approximately the same final temperatures were reached in the insulated cases (A5 – LWC, B2 – insulation inside and D2 – steel insulation outside), see Figure 11. The maximum temperature which can be computed from Eq. (43) (approximately 1200 $^{\circ}$C) agreed very well with the maximum measured temperature during the experiments. However, the time history to reach the final temperature is very different between these cases. The relatively high density of the LWC requires a long time to reach final temperature, whereas in the B-series, the insulation inside the enclosure reaches final temperatures after only a few minutes. When the insulation is on the outside of the steel, the inertia of the fire exposed steel significantly delays the time to reach equilibrium. With uninsulated steel, the final temperature is several hundred degrees lower than the final temperatures of all the other cases.

Fire temperatures numerically calculated by using the new model have been compared with experimentally measured temperatures for two fire experiments conducted in the compartment with moist (Test A1) and dry light weight concrete (Test A5) boundaries, respectively, see (Byström, et al., 2015). Good agreement between measured and calculated temperatures was obtained as shown in Figure 12 for both the original and the dry LWC. However, parametric fire curve temperatures according to EN 1991-1-2 overestimates the fire temperature increase after 10 minutes, see Figure 12. Note that the effect of moisture evaporation on the temperature development is considered very accurately by numerical calculation, see Figure 12. The moisture content makes the temperature development rate slower.

Figure 11. Experimental results of the light weight concrete tests: A1 and A5; the Insulated steel tests: on the inside -B2 and outside -D2, Uninsulated steel tests – C2. These results show compartment mean, maximum and minimum temperatures measured with PTs.

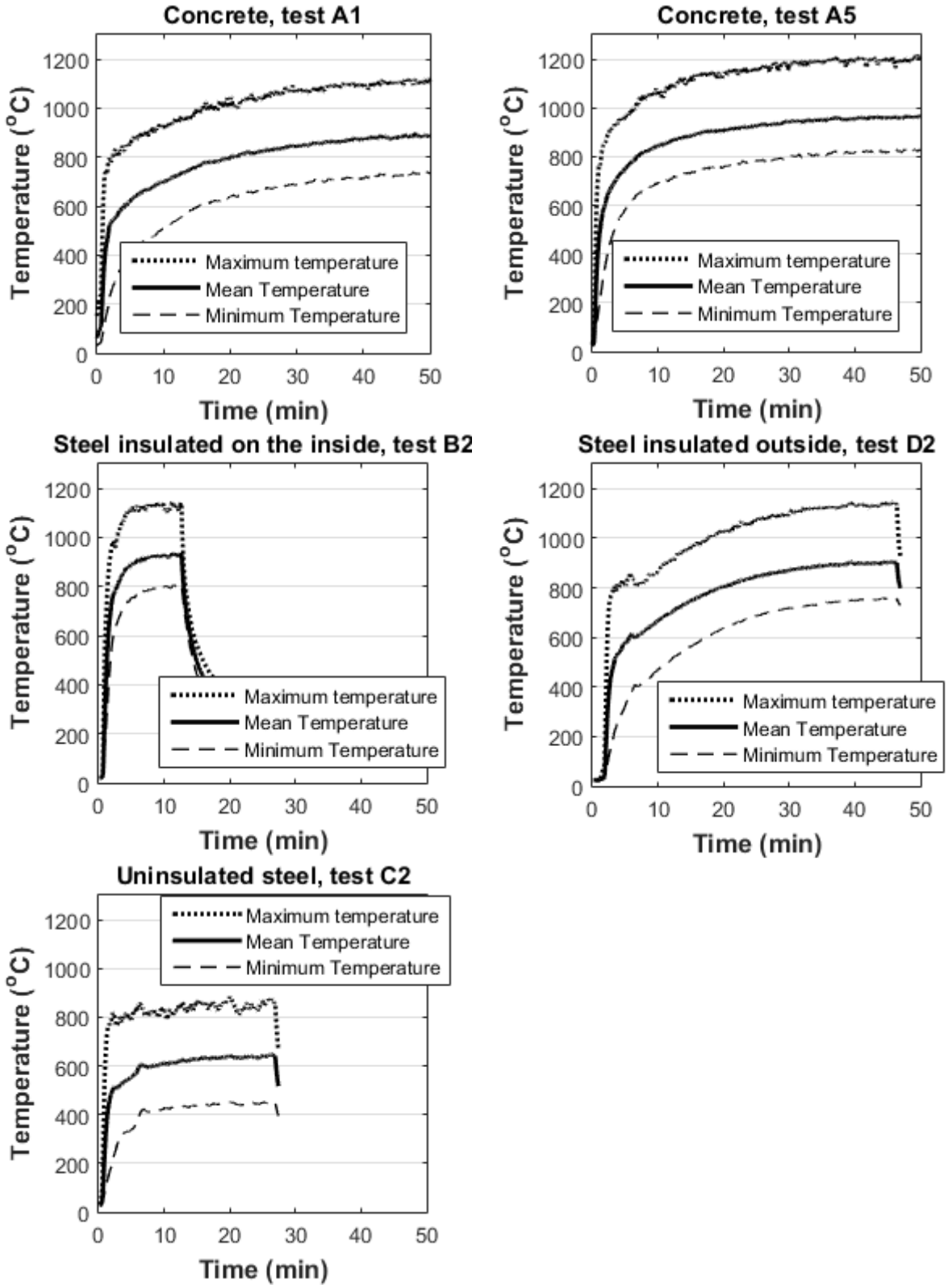

Figure 12. Left: Comparison of calculated and measured temperature. Right: Dry concrete: experimental measured temperature vs. calculated with new model and EN 1991-1-2 ($\Gamma = 15.5$, see Appendix A)

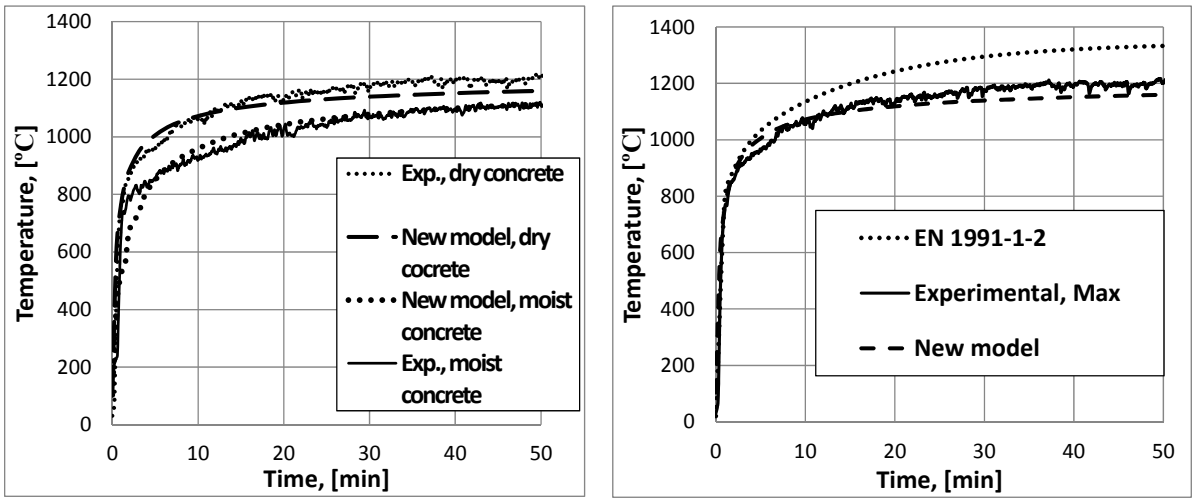

Figure 13. Measured and calculated fire temperatures in fully developed compartment fire in a steel sheet compartment.

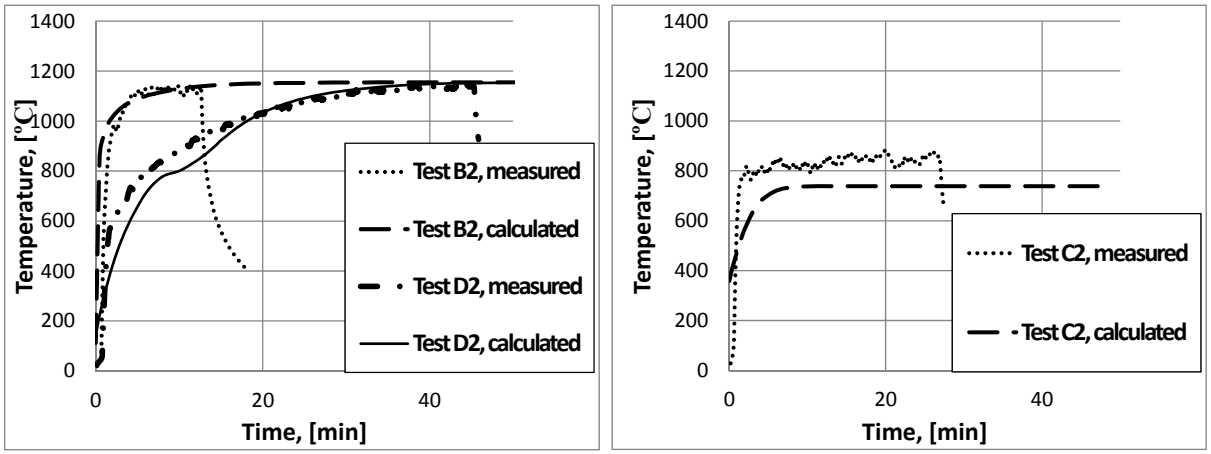

The same type of calculation was done for the steel sheet compartment without insulation (Test C2) and with insulation on inside (Test B2) and outside (Test D2), respectively. The calculated fire temperatures with the new model were compared with measured maximum temperatures. The material properties of the insulation and the LWC were assumed temperature dependent. Good agreement with the measured values and calculated temperatures were obtained as shown in Figure 13. Observe that the fire temperature of the steel compartment with insulation on the inside tends much faster to the maximum temperature than when the insulation is on the outside.

The fire temperature reaches about 1200 °C (T_{max}) during the test A, test B and Test D, see Figure 12 and Figure 13, while for the non-insulated case the final temperature reaches only around 800 °C.

Note that this calculation model yields exceptionally good predictions particular in terms of the qualitative development of the fire temperature, i.e. the maximum temperatures are accurately predicted and temperature rise rates well predicted.

7. Conclusions

In this report a new simple computational model has been validated with experiments conducted in compartments of light weight concrete and steel insulated on the outside and on the inside as well as non-insulated. The use of FE analysis gives the opportunity to very well predict fire temperature considering combinations of materials and non-linearities like material properties varying with temperature and moisture content (latent heat).

Some overall conclusions can be made:

- The fire temperature calculated with the new model is in good agreement with the highest measured temperatures.
- The effects of moisture in the boundary structure (Test A1) are predicted very well by the numerical calculations.
- The parametric fire temperature curves calculated according to EN 1991-1-2 over estimated the temperature for the LWC structure. These curves cannot be used for the steel sheet cases, see Appendix A.
- The calculation model yields exceptionally good predictions particularly in terms of the qualitative development of the fire temperature

- In addition: overall temperature predicted with FDS analysis (Appendix B) agreed well the measured temperature from the test A5 and C2.

Bibliography

Babrauskas, V., 1996. Fire Modelling Tools for Fire Safety Engineering: are they good enough?. *Journal of Fire Protection Engineering,* pp. Vol. 8, No. 2, 87-96.

Byström, A., 2013. *Fire temperature development in enclosures: Some theoretical and experimental studies.* Luleå, Sweden: Luleå University of Technology.

Byström, A., Sjöström, J. & Wickström , U., 2015. *Influence of surrounding boundaries on fire compartment temperature.* Dubrovnik, s.n., pp. 386-391.

Byström, A., Sjöström, J. & Wickström, U., 2016. *Temperature Measurements and Modelling of Flashed Over Compartment Fires.* Royal Holloway College, Nr Windsor, UK, Proceedings of the 14th International Conference and Exhibition on Fire Science and Engineering, Interflam.

Drysdale, D., 1998. *An introduction to fire dynamics. Second edition.* s.l.:John.

Evegren, F. & Wickström, U., 2015. New approach to estimate temperatures in pre-flashover fires: Lumped heat case. *Fire Safety Journal,* pp. 77-86.

Harmathy, T. Z., 1972. A new look at compartment fires, Part I. *Fire Technology,* pp. Vol. 2, No. 2, 196-217.

Harmathy, T. Z., 1972. A new look at compartment fires, Part II. *Fire Technology,* pp. Vol. 8, No. 4, 326-351.

Holman, J. P., 2010. *Heat Transfer, Tenth Edition.* s.l.:McGraw-Hill Publisher.

Hunt, S. P. & Cutonilli, J., 2010. *Evaluation of Enclosure Temperature Empirical Models,* s.l.: Society Of Fire Protection Engineers Technical Reports.

Hurley, M. J., 2005. Evaluation of models of fully developed post-falshover compartment fires.. *Journal Of Fire Protection Engineering, Vol 15,* pp. 173-197.

Jansson, R. & Anderson, J., 2012. *Experimental and numerical investigation of fire dynamics in a fasade test rig.*. Santander, Fire Computer Modelling.

Jones, W. W., 1983. *A Review of Compartment Fire Models PB-83-208173,* Gaithersburg: National Bureau of Standards.

Kawagoe, K., 1958. *Fire behaviour in rooms. Report 27.,* s.l.: Building Research Institute of Japan.

Lie, T. T., 2002. *Fire temperature-time relationships,* Quincy, Massachusetts: National Protection Association : Protection Engineering, Third Edition.

Magnusson, S. E. & Thelandersson, S., 1970. *Temperature-Time Curves of Complete Process of Fire Development.* Stockholm: s.n.

Magnusson, S. E. & Thelandersson, S., 1974. A Discussion of Compartment Fires. *Fire Technology, Vol. 10 (3),* pp. 228-246.

Ma, Z. & Mäkeläinen, P., 2000. Parametric Temperature-Time Curves of Medium Compartment Fires for Structural Design. *Fire Safety Journal,* pp. Vol. 34, 361-375.

McGrattan, K. B., Baum, H. R. & Rehm, R. G., 1998. Large eddy simulations of smoke movement. *Fire Safety Journal,* Volume 30, pp. 161-178.

McGrattan, K. et al., 2013. *Fire Dynamics Simulator. User's Guide. Special Publication 1019: Sixth Edition,* s.l.: National Institute of Standards and Technology, NIST.

Mowrer, F. W., 1992. Closed-Form Estimate of Fire-Induced Ventilation Through Single Rectangular Wall Openings,. *Journal of Fire Protection Engineering,* pp. 105-116.

Pettersson, O., Magnusson, S. & Thor, J., 1976. *Fire Engineering Design of Steel Structures,* Stockholm: Swedish Institute of Steel Construction, Publication No. 50.

Sjöström, J. & Anderson, P., 2013. *SP Report 2013:61 Thermal exposure from burning leaks on LNG hoses: experimental results,* Borås: SP Technical Research Institute of Sweden.

Sjöström, J., Appel, G., Amon, F. & Persson, H., 2013. *SP 2013:02 ETANKFIRE – Large scale burning behaviour,* Borås: SP Technical Research Institute of Sweden.

Sjöström, J. & Wickström, U., 2013. *Different types of Plate Thermometers for measuring incident radiant heat flux and adiabatic surface temperature.* London, Interscience Communications Ltd, p. 363.

Sjöström, J. & Wickström, U., 2015. *Data from experiments at Research Gate.* [Online].

Sjöström, J., Wickström, U. & Byström, A., 2016. *SP Report 2016:54. Validation data for room fire models: Experimental background,* Borås: SP Technical Research Institute of Sweden.

Sundström, O. & Gustavsson, S., 2012. *Simple temperature calculation models for compartment fires,* Luleå, Sweden: Bachelor's thesis, Luleå University of Technology.

Thomas, P. H. & Heselden, A., 1972. *Fully Developed Fires in Single Compartment. A Co-operative research program of the Conseil International du Batiment (CIB Report No.20),* Borehamwood, UK: Fire Research Note No.923, Fire Research Station.

Wade, C. A., 2008. *BRANZFIRE 2008 Compilaition of Verification Data,* Porirua: Branz.

Wickström, U., 1979. *TASEF-2 – A Computer Program for Temperature Analysis of Structures Exposed to Fire,* Lund: Lund Institute of Technology, Department of Structural Mechanics.

Wickström, U., 1985. Applications of the standards fire curve for expressing natural fires for design purposes.. *Fire Safety: Science and Engineering. ASTM STP 882, American Society for Testing and Materials, Philadelphia,* pp. 145-159.

Wickström, U., 2016. *Temperature Calculation in Fire Safety Engineering. 1st Edition.*. 1 ed. Verlag: Springer International Publishing.

Wickström, U. & Byström, A., 2014. Compartment fire temperature: a new simple calculation method. *IAFSS - The International Association for Fire Safety Science : proceedings,* pp. 289-301.

Appendix A - Thermal action according to Eurocode (EN 1991-1-2)

According to EN 1991-1-2, the temperature-time curve in the heating phase in the compartment, can be written as:

$$T_f = 20 + 1325 \cdot \left(1 - 0.324 \cdot e^{-0.2 \cdot t^*} - 0.204 \cdot e^{-1.7 \cdot t^*} - 0.472 \cdot e^{-19 \cdot t^*}\right) \quad \text{(A1)}$$

where the dimensionless time, t^*, depends on the opening dimensions and compartment boundaries: the thermal conductivity, k ; the density, ρ and the specific heat capacity, c, i.e.:

$$t^* = t \cdot \Gamma \quad \text{(A2)}$$

where time t is in minutes. Γ is named the time factor, a function of the opening factor O, given in Eq. (11), and the thermal inertia $\sqrt{k\rho c}$

$$\Gamma = \left[\frac{O / \sqrt{k \cdot \rho \cdot c}}{0.04 / 1160} \right]^2 \quad \text{(A3)}$$

with the following limits: $100 \le \rho c \lambda \le 2200$, [J/m^{2}s$^{1/2}$K]

and where ρ is the density of boundary of enclosure, [kg/m^3]; c is specific heat of boundary of enclosure, [J/kgK]; λ thermal conductivity of boundary of enclosure, [W/mK]; $O = \frac{A_v \sqrt{h_{eq}}}{A_t}$ - opening factor with the following limits $0.02 \le O \le 0.20$

Appendix B (by Johan Anderson) – Simulation results: temperature calculated by FDS vs measured temperature

The simulations are performed using the Fire dynamics Simulator (FDS) version 6.0 (McGrattan, et al., 2013). The FDS software solves the Navier-Stokes equations in the limit of low-speed, thermally-driven flow with an emphasis on smoke and heat transport from fires. The algorithm used is an explicit predictor-corrector scheme that is second order accurate in space and time where turbulence is treated by means of Large Eddy Simulation (LES). The FDS software with default settings uses structured, uniform staggered grid in order to utilize the efficiency of the Fast Fourier transforms in the pressure solver. The combustion chemistry is simplified and a generalized lumped species approach together with the eddy dissipation concept is used for a single step reaction between fuel and oxidizer. In the default setting radiation is calculated using 100 discrete angles in a finite volume approximation of the radiation transport equation with grey gas. The FDS model is not limited to these simple algorithms however any additional physics included incur increased computational costs. The default model options have been selected based on results from a wide variety of full-scale validation experiments (McGrattan, et al., 2013).

In this work the simulations are done in accordance with the tests using the same heat release rates and geometrical set-up and extracting similar outputs as in the experimental scenarios described early, (Sjöström, et al., 2016). The simulations have been focused on two cases with light weight concrete (LWC) and un-insulated steel. The material data is taken from data sheets and measurements. Although the steady-state simulations (constant heat release rate) only simulate 2000s of fire we find that steady-state temperatures are reached in all cases. In the model a propane diffusion burner is introduced that supplies the required heat release rates. The plate thermometers are introduced as physical objects in the simulation to be able to account for the time constant of the insulating material and the sheet of metal in the plate thermometer, the model is described in (Jansson & Anderson, 2012).

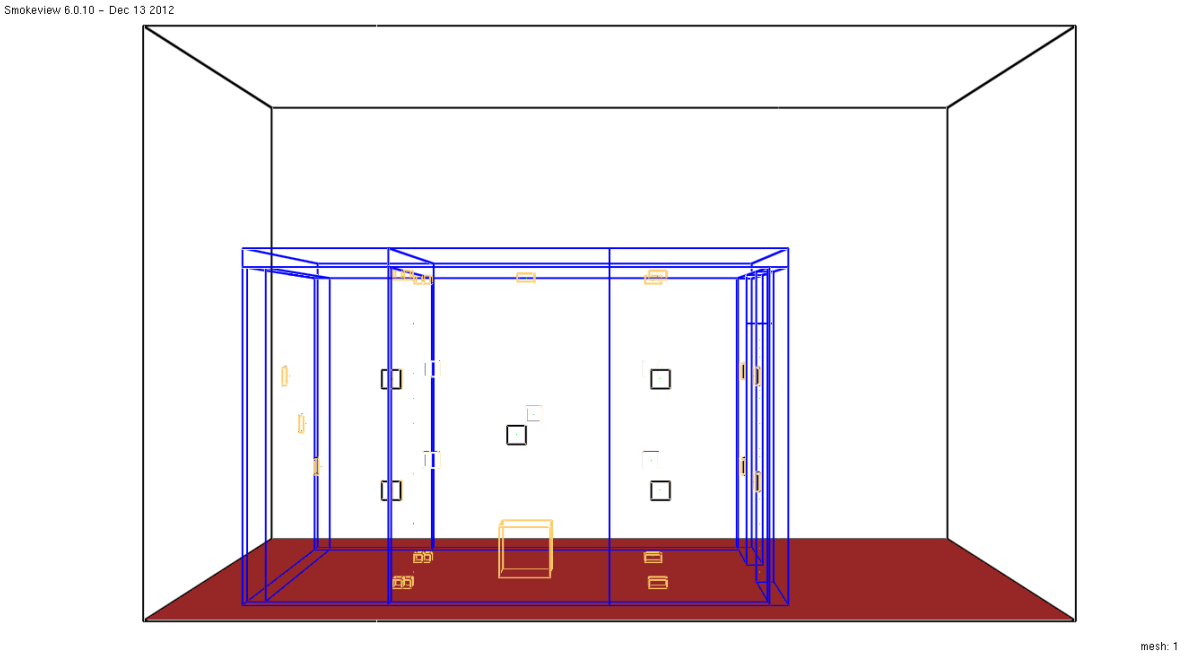

Figure 14 The physical geometry used in the simulations including the placement of the burner and the plate thermometers

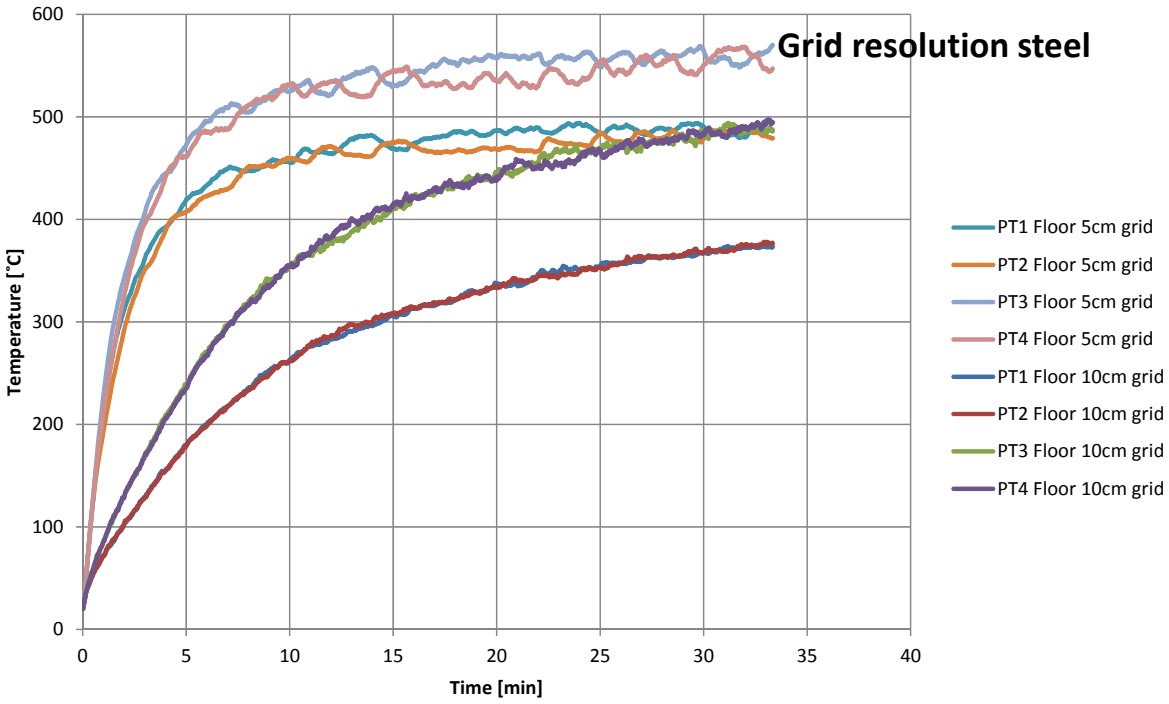

Figure 15 Grid resolution test displayed for the plate thermometers on the floor.

Three mesh resolutions are tested in order to check the numerical stability of the results. The mesh is cubic rectilinear staggered grids with resolutions of 2.5cm, 5.0cm and 10cm. In Figure 14, the geometry of the simulation domain is given including the placements of the plate thermometers and the propane burner. An indication of the needed resolutions is the value of $D^*/\delta x > 10$, where $D^*=0.882$. We find that a grid resolution of 10cm gives $D^*/\delta x=8.8$, 5cm gives $D^*/\delta x=17.6$ and finally 2.5cm yields $D^*/\delta x=35.3$. This indicates that

5cm grid should be sufficient to resolve the fire load. The result of the grid resolution test is displayed in Figure 15 for the temperatures registered by the plate thermometers on the floor. It is found that the growth rate of the temperature is quite significantly dependent on the grid resolution whereas the final temperatures are less dependent, in a comparison between 5cm and 10cm grids. A similar result was found for the LWC case. The results from the 2.5cm grid are approximately the same as the results from 5cm grid. In the remainder of the report a resolution of 5cm will be used.

In general, the simulations have been streamlined to assume as many of the standard default values as possible in the simulations as is usually done by consultancy.

A series – LWC –Test A5 - 1000 kW.

The A series is performed using measured values of the thermal properties of the LWC, see Table 4. In order to investigate the importance of the input data a small sensitivity analysis was performed where the density, heat conductivity and the specific heat was varied by ±10%.The result of the sensitivity study was that moderate changes to the input values only had very small differences in the simulated temperatures on the plate thermometers and the thermo couples in the door. A few specific comparisons between the simulated case and the experimental data are made to assess the viability of modelling the room fire scenario with the FDS software. The comparisons for the LWC cases are shown in Figure 16 to Figure 19. Although the measurement data showed that an asymmetry between left and right wall data was present the numerical simulations are done without this particular complication.

In Figure 16, the thermocouple measured data is compared to the simulation data and good agreement is found over the whole height of the door. However, it seems that the simulated case is on the lower side comparing the plate thermometers at the floor, see Figure 17. On the left wall a good agreement is found displayed in Figure 18 and again lower temperatures are found in the simulations compared to the measured data with the plate thermometers on the ceiling. There are a number of reasons for these discrepancies among them are the uncertainty of the moisture content in the walls and the effect of the modified plate thermometers with thicker insulation material on the back. Also in this type of room the radiative fraction is rather unknown which could influence on the radiation – convection balance that determines the actual temperature on the plate thermometers.

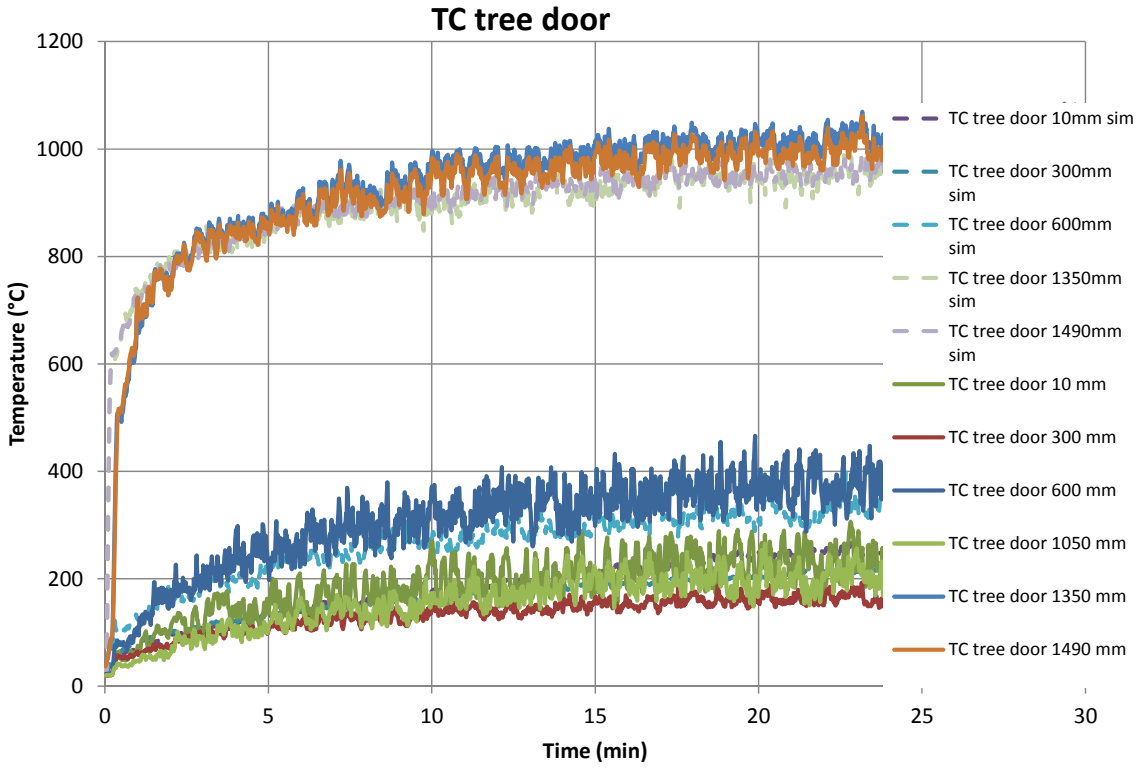

Figure 16 TC tree in the door at different heights.

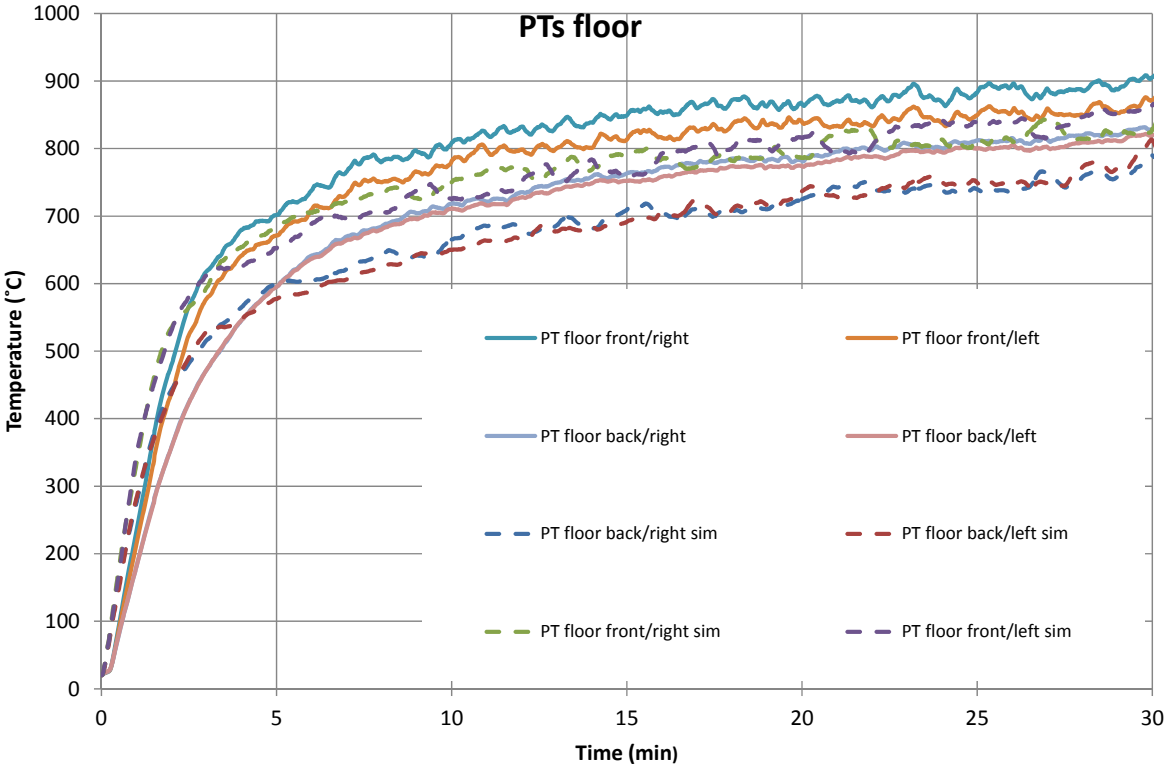

Figure 17 Plate thermometers on the floor.

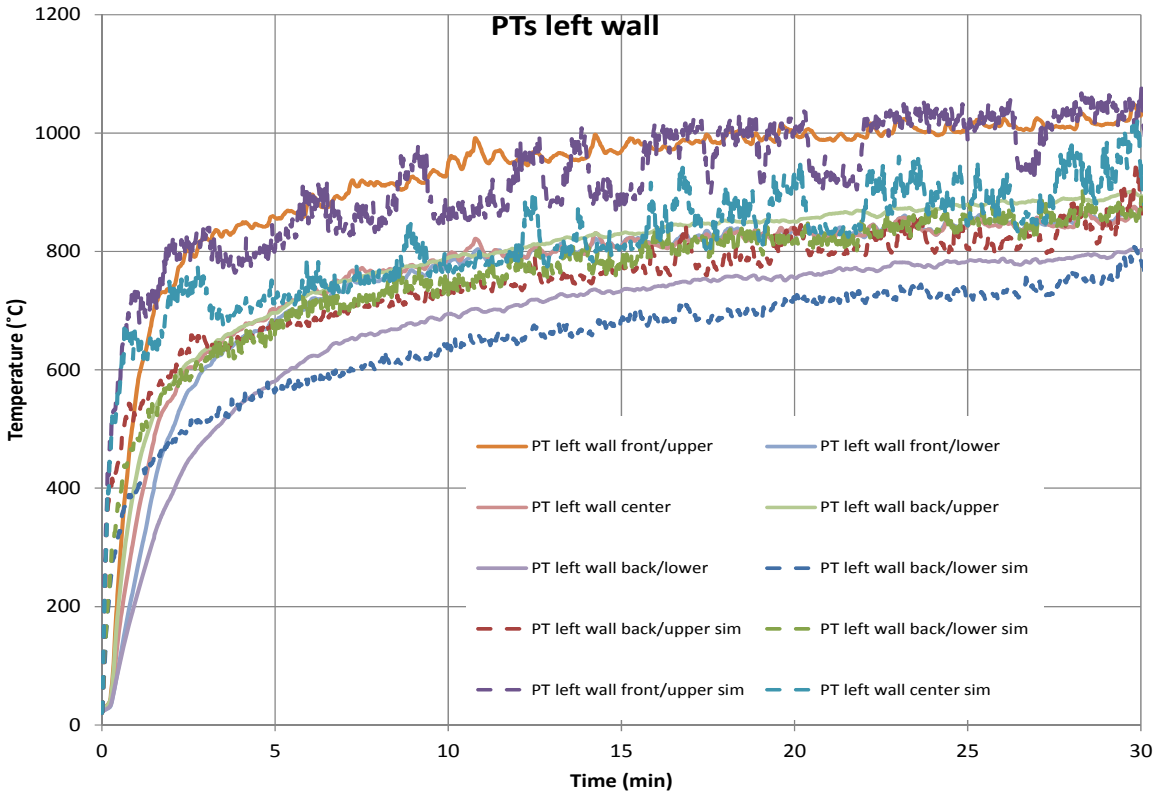

Figure 18 Plate thermometers on the left wall.

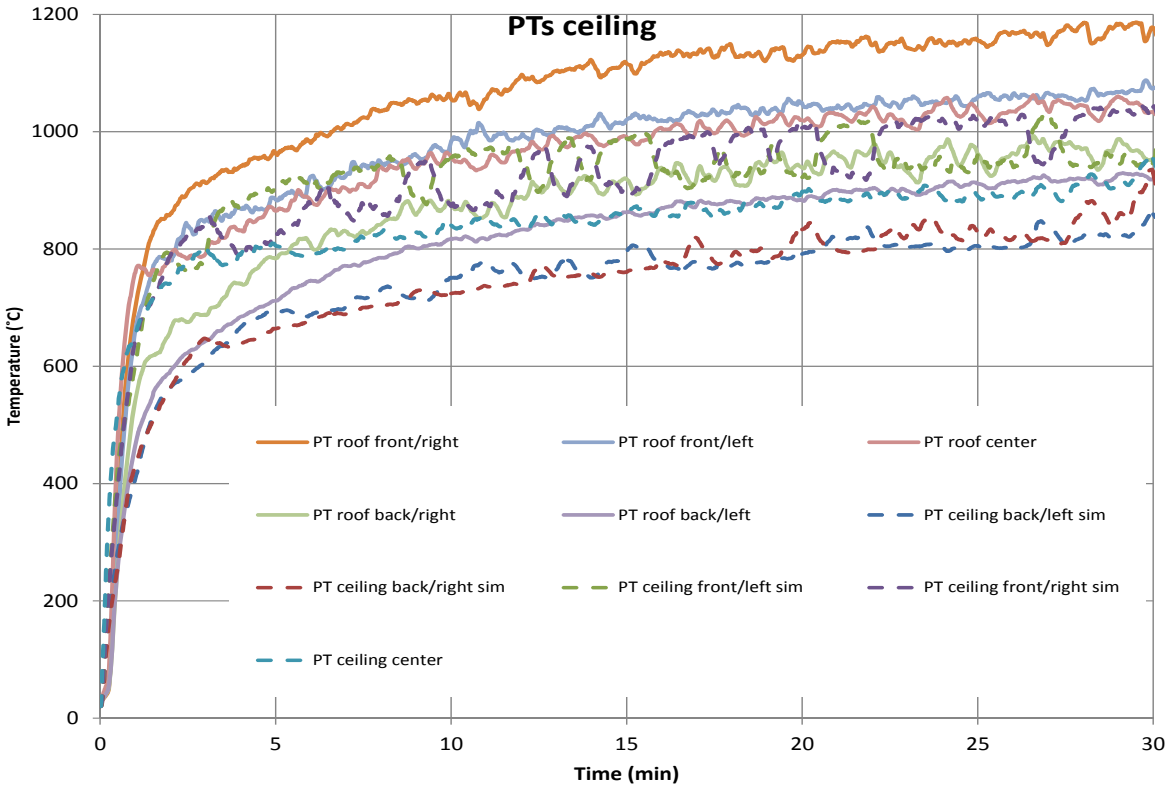

Figure 19 Plate thermometers on the ceiling.

C series – steel un-insulated –Test C2 - 1000 kW

In the C series a room with the same dimensions as in the A series however it is built with 3mm steel plate. The thermal material data is taken from Inconel as shown in Table 6.

Table 6 Thermal data for the Inconel steel

Material name	Density (ρ) [kg/m^3]	Heat conductivity (k) [W/mK]	Specific heat (C_p) [kJ/mK]
Inconel	8430	14.9 (at 20˚C)	0.4 (at 20˚C)
		25.0 (at 727˚C)	0.6 (at 727˚C)

Note that the heat conductivity and specific heat varies with temperature which is taken into account by linear interpolation as indicated in Table 6.

The comparisons are shown in Figure 20 to Figure 23. In Figure 20, the thermocouple data is compared to the simulated data and in general a good agreement is found. The simulated temperatures by the plate thermometers on the floor show very good agreement with the measured data as shown in Figure 21, indicating that the radiation from the fire and the ceiling is correctly captured in the simulation. In Figure 22 and Figure 23, comparisons between the measured temperatures by the plate thermometers and the simulated temperatures display a good agreement over the whole simulation time. In general, the simulation data in the C series are representing the measured data to much higher degree compared to the A series. This is due to the much simpler system consisting only of steel plate and the dynamics of a well specified fire source.

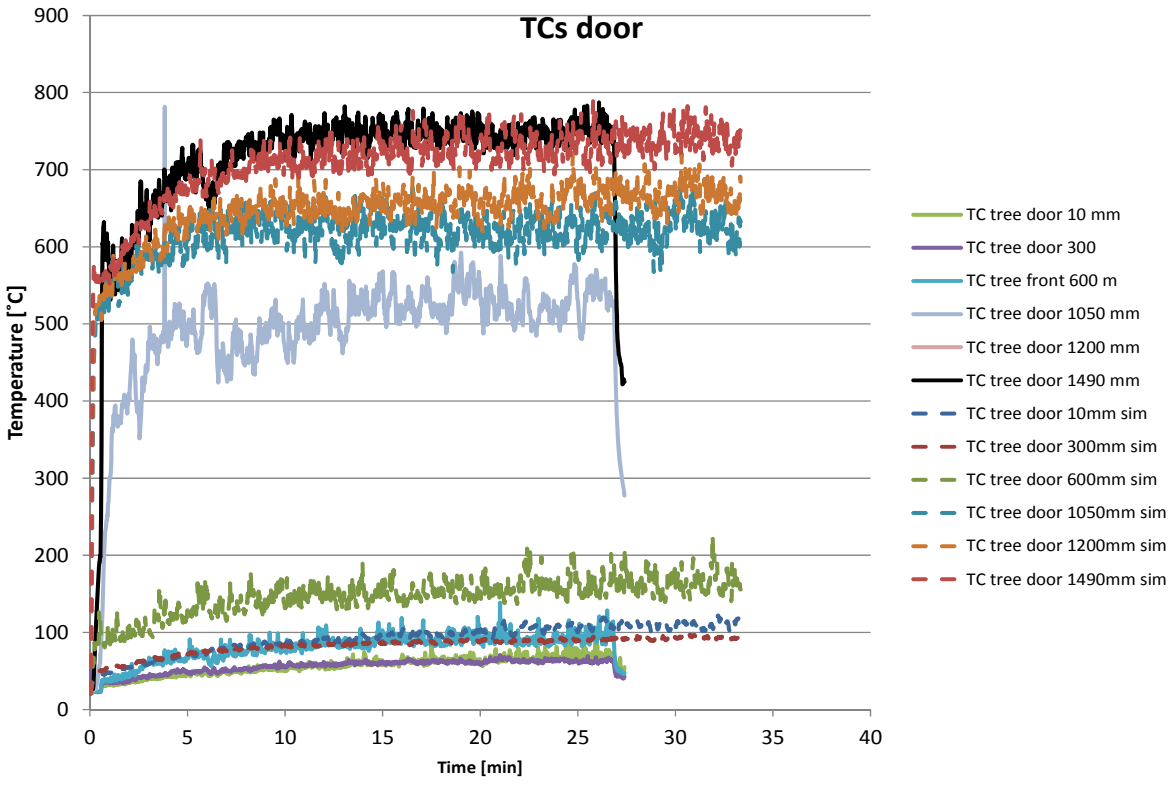

Figure 20 TCs in the door

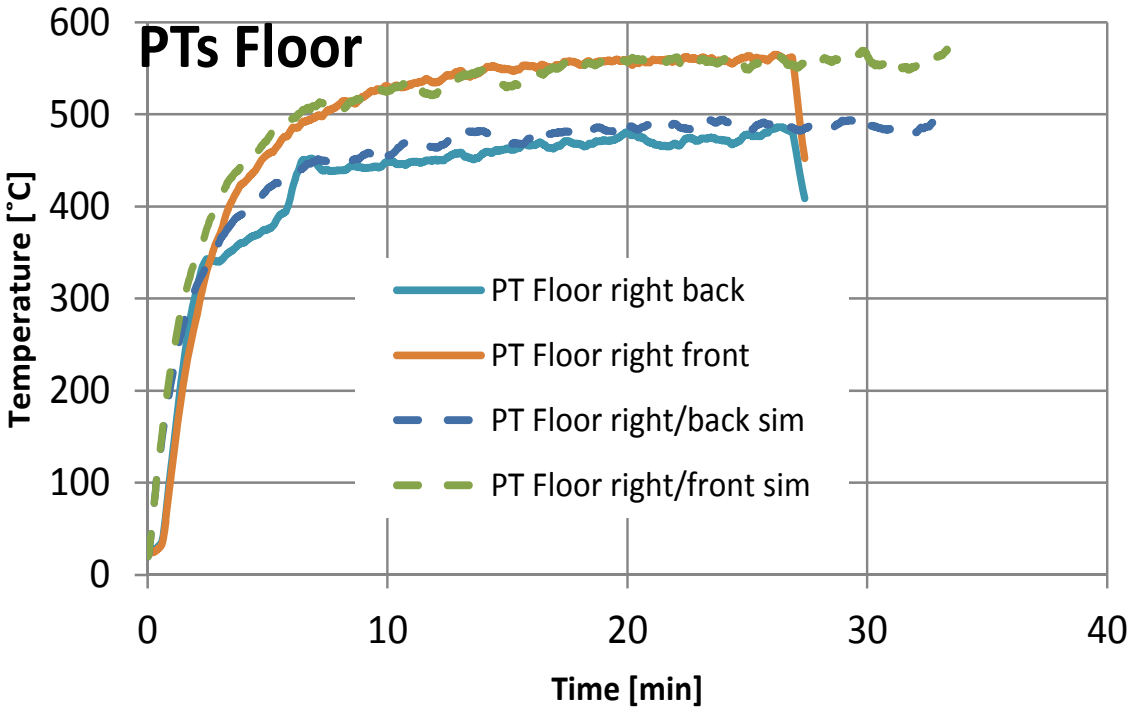

Figure 21 Plate thermometers on the floor.

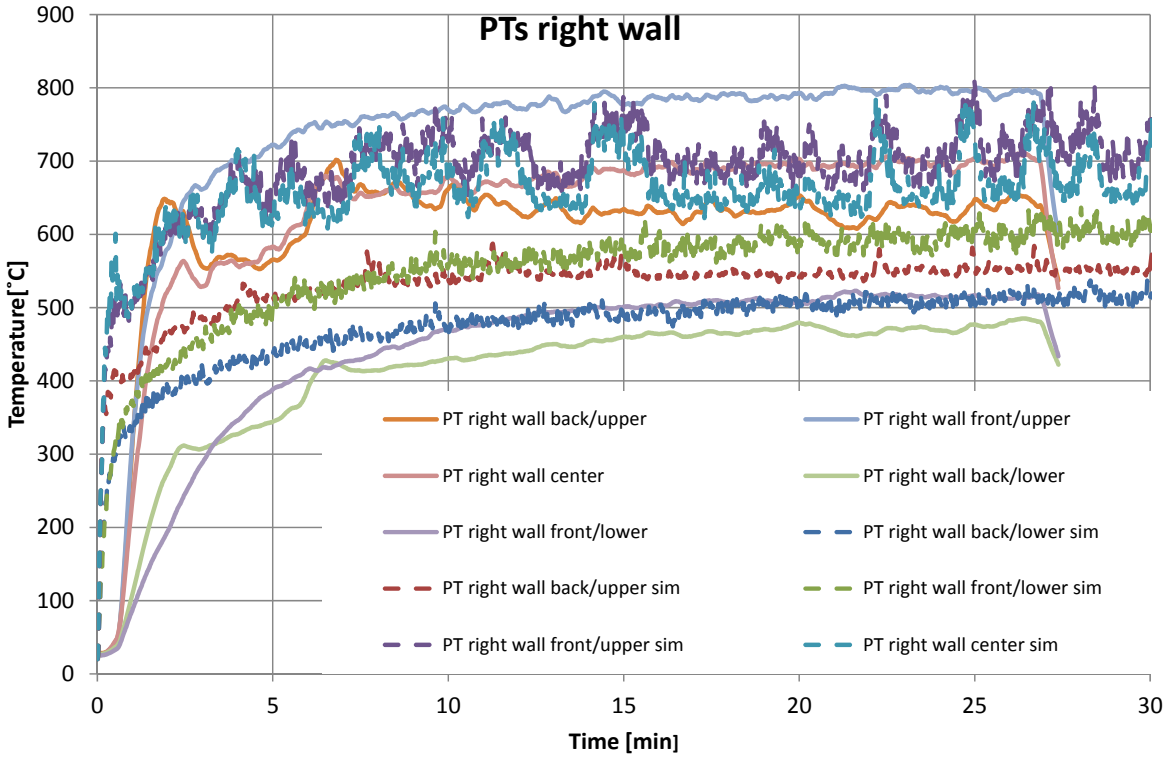

Figure 22 Plate thermometers on the right wall.

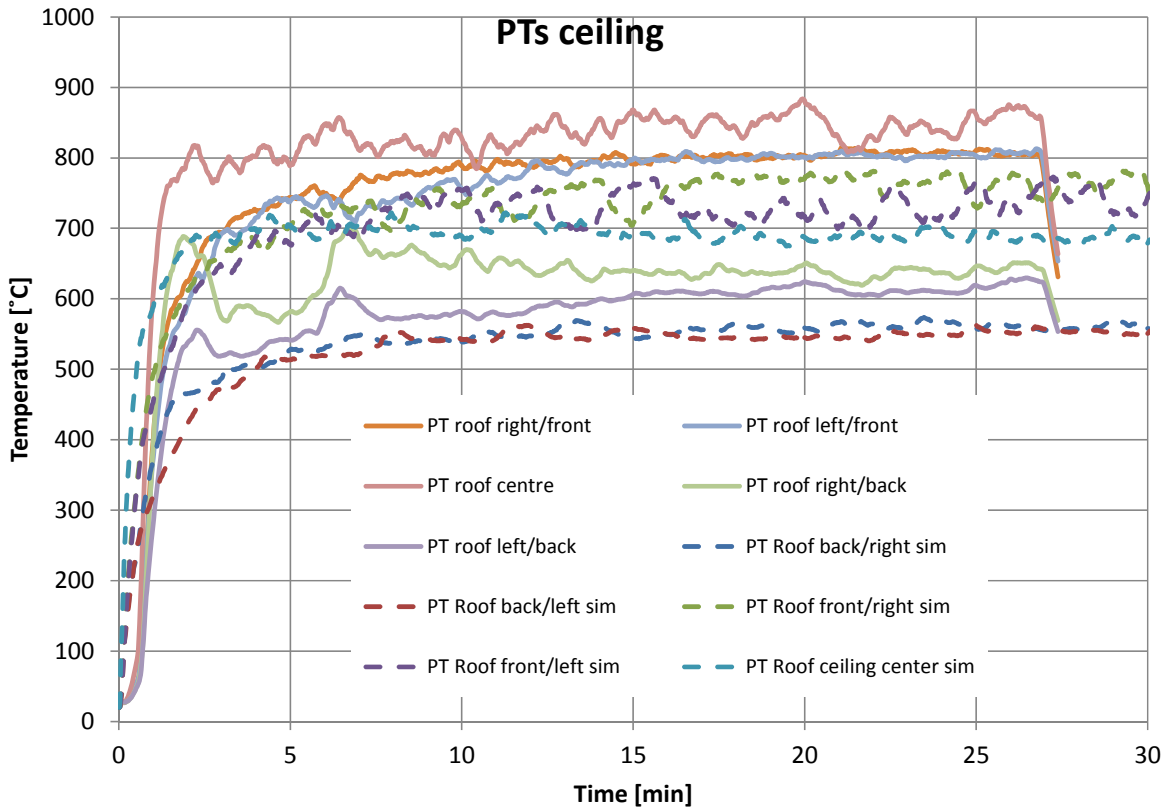

Figure 23 Plate thermometers on the ceiling.

Appendix C – Results from numerical simulation

Case A – Lightweight concrete compartment boundaries

Two experiments have been selected and compared:

- The first experiment, TEST A1, was conducted in the compartment with the structures containing its original moisture. The density of the material was measured before testing to be around 760 kg/m^3 containing 39 % of moisture (dry basis by weight).
- The second experiment was conducted in the same compartment after a series of fire experiments, TEST A5. So it can be assumed that the concrete had dried out after 5 days of experiments.

More details for the original concrete as well as after exposure in a furnace of 105 °C during 24 h are found in Table 4.

Assumptions for FE analysis:

- Due to limitation of the software the heat transfer resistance between the fire gases and the exposed surface is kept at the constant values of
  - $R_{i.tot} = 1/h_{i.tot} = 1/200$ [m^{2}K/W], for $T_f = T_s = 650$ [°C]
  - $R_{i.tot} = 1/h_{i.tot} = 1/300$ [m^{2}K/W], for $T_f = T_s = 850$ [°C]
  - $R_{i.tot} = 1/h_{i.tot} = 1/450$ [m^{2}K/W], for $T_f = T_s = 1000$ [°C]

  (see Figure 24), where $R_{i.tot}$ in the figure denotes the total heat transfer thermal resistance at the fire exposed surface (for the mixed boundary condition, i.e. both radiation, $R_{i.r}$, and convection heat transfer, $R_{i.c}$), see Eq. (22).

  The convection heat transfer coefficient is assumed to be $h_{i.c}$, 30 [W/m^{2}K] and radiation heat transfer coefficient, $h_{i.r} = 4\varepsilon\sigma T_r^3$, for $T_f = T_s = 650$ [°C], $T_f = T_s = 850$ [°C] and $T_f = T_s = 1000$ [°C] respectively.
- The heat transfer coefficient by convection on the unexposed side was assumed equal to 4 W/m^{2}K
- The emissivities of the light weight concrete surfaces were assumed equal to 0.9 both on exposed and the unexposed sides.

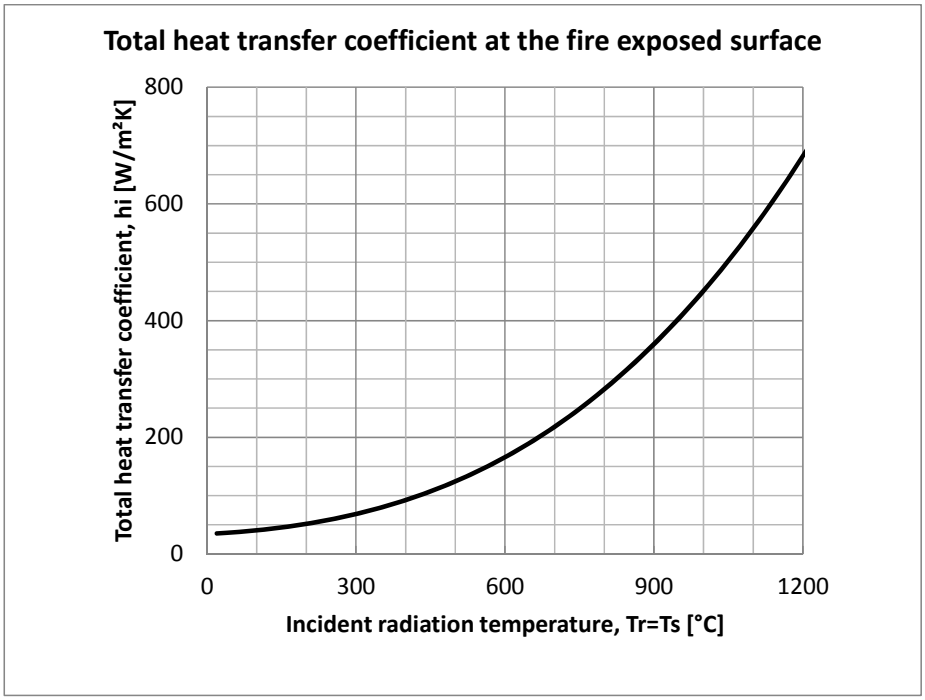

Figure 24. Heat transfer coefficient for the fire exposed surface

Fire temperatures numerically calculated by using the new model have been compared with experimentally measured temperatures for two fire experiments conducted in the compartment with moist (Figure 25) and dry light weight concrete boundaries (Figure 26), respectively.

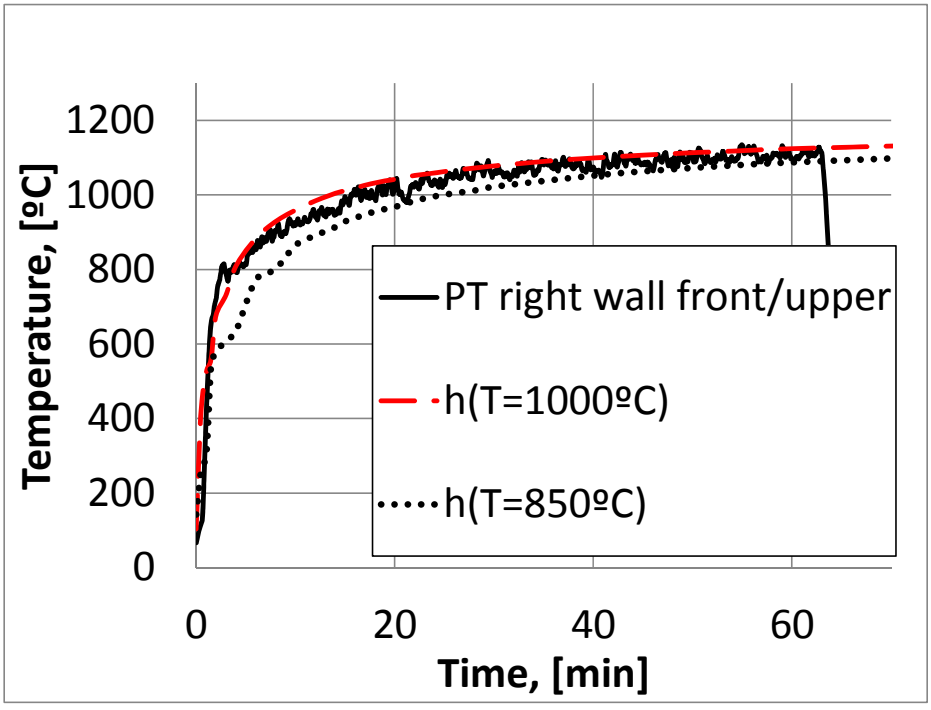

Figure 25. Comparison of calculated temperatures with measured higher temperature during experiments – Case A1.

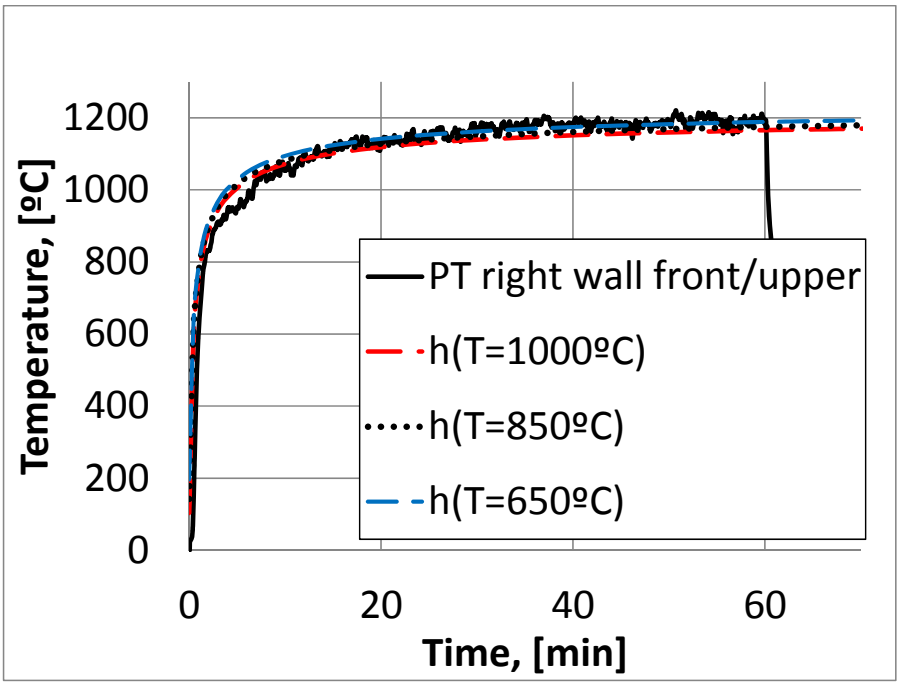

Figure 26. Comparison of calculated temperatures with measured higher temperature during experiments – Case A5.

As we can see on the Figure 25 and Figure 26, the fire temperature goes above 1000 °C rather fast, so the assumption of the heat transfer resistance between the fire gases and the exposed surface is kept at the constant values of $R_{i.tot} = 1/h_{i.tot} = 1/450$ [m^{2}K/W], for $T_f = T_s = 1000$ [°C] can be quite reasonable and have been used for analysis, see Figure 27.

Note that the effect of moisture evaporation on the temperature development is handled very accurately by numerical calculation, see Figure 27 a). The moisture content makes the temperature development rate slower.

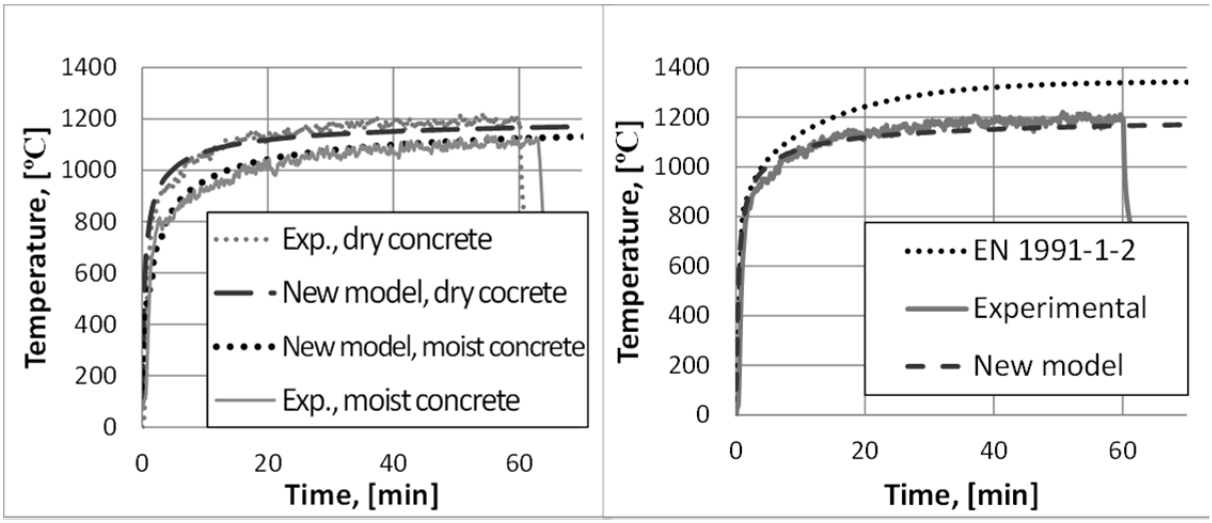

a) Experimental measured temperatures vs. calculated ones

b) Dry concrete: experimental measured temperature vs. calculated with new model and EN 1991-1-2 ($\Gamma = 15.5$, Eq. (A1))

Figure 27. Comparison of calculated temperatures with measured higher temperature during experiments

Case B – steel structure insulated on the inside

Two experiments with the highest HRR (1000kW) so called B1 and B2 has been validated with calculated temperatures. Since the highest measured temperature and the temperature increase during those experiments was the same, only one of them (B2) has been validated to the calculated temperatures.

Test series B was conducted on a steel structure with 3 mm thickness, for more details see (Sjöström, et al., 2016). The inner dimensions of the steel enclosure were identical to test series A. However, 50 mm of stone wool board covered the inside walls. Thus, the width/length/height of the inner surfaces in test series B are 100 mm smaller compared to series A, giving dimensions of 1700/2600/1700 mm, respectively.

The stone wool had a nominal density of 200 kg/m^3 and a nominal room temperature conductivity of 0.04 W/m K, see Table 7. The conductivity values for stone wool are taking for KIMMCO insulation board up to 350 °C. Up to 1200 °C the value of conductivity were extrapolated, see Figure 10.

Table 7 Thermal material properties of the steel and stone wool used in FE analysis

Material properties	**Density, [kg/m3]**	**Specific heat capacity, [J/(kg K)]**	**Conductivity, [W/(m K)]**
According to	7850	C(T)	k(T)
Stone wool	200	0.83	k(T), see **Error! Reference source not found.**

Assumptions:

- The heat transfer resistance between the fire gases and the exposed surface is kept constant:
  - o $R_{i.tot} = 1/h_{i.tot} = 1/300$ [m^{2}K/W], for $T_f = T_s = 850$ [°C]
  - o $R_{i.tot} = 1/h_{i.tot} = 1/450$ [m^{2}K/W], for $T_f = T_s = 1000$ [°C]

  (see Figure 24), where the convection heat transfer coefficient is assumed of $h_{i.c}$, 30 [W/m^{2}K] and radiation heat transfer coefficient, $h_{i.r} = 4\varepsilon\sigma T_r^3$, for $T_f = T_s = 850$ [°C] and $T_f = T_s = 1000$ [°C] respectively.
- The heat transfer coefficient by convection on the unexposed side was assumed equal to 4 W/m^{2}K, according the to the EC1 recommendations
- The emissivities of surfaces were assumed equal to 0.9 both on exposed and the unexposed sides.

Fire temperatures numerically calculated by using the new model have been compared with experimentally measured temperatures conducted in the compartment with non-insulated steel boundaries. Good agreement with the measured values and calculated temperatures were obtained as shown in Figure 28.

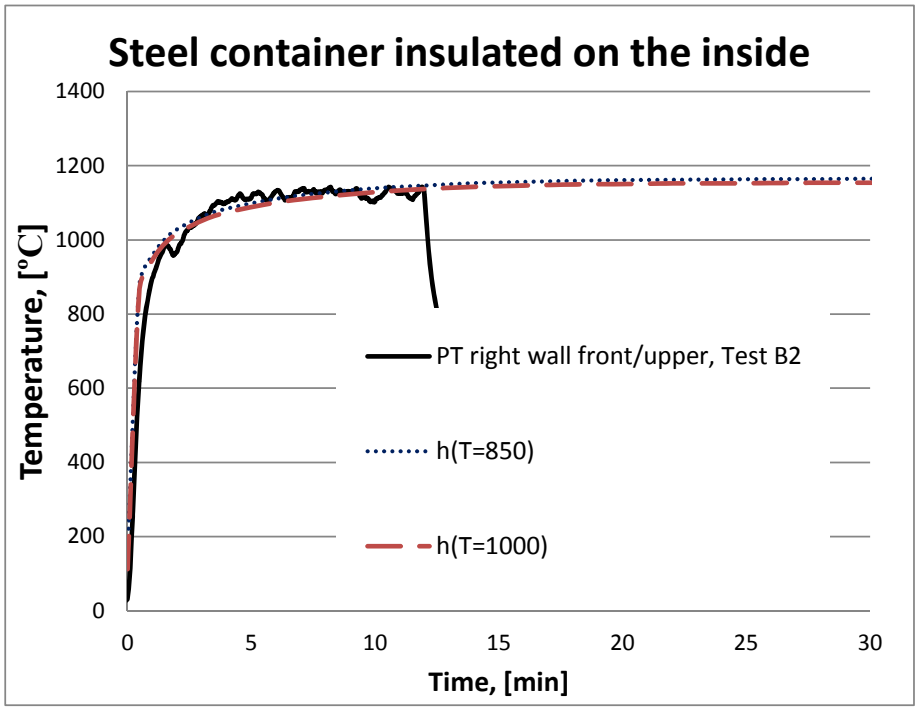

Figure 28. Comparison of calculated temperatures with measured higher temperature during experiments: Experimental measured temperatures with PT vs. calculated ones with Tasef. Insulated on the inside steel container

As we can see on the Figure 28, the fire temperature goes above 1000 °C rather fast, so the assumption of the heat transfer resistance between the fire gases and the exposed surface is kept at the constant values of $R_{i.tot} = 1/h_{i.tot} = 1/450$ [m^{2}K/W], for $T_f = T_s = 1000$ [°C] can be quite reasonable and have been used for analysis, see Figure 13.

Case C – Un-insulated steel compartment boundaries

The experiment with the highest HRR (1000kW) so called C2 has been selected and compared.

The thickness of the walls was 3mm. The material properties of the steel, see Table 8.

Table 8 Thermal material properties of the steel.

Material properties	Density, [kg/m3]	Specific heat capacity, [J/(kg K)]	Conductivity, [W/(m K)]
According to EC4	7850	C(T)	k(T)
Constant steel properties, independent on the temperature of the material	7850	480	46

Assumptions:

- The heat transfer resistance between the fire gases and the exposed surface is kept constant:
  - $R_{i.tot} = 1/h_{i.tot} = 1/92$ [m^{2}K/W], for $T_f = T_s = 400$ [°C]
  - $R_{i.tot} = 1/h_{i.tot} = 1/166$ [m^{2}K/W], for $T_f = T_s = 600$ [°C]

  (see Figure 24), where the convection heat transfer coefficient is assumed of $h_{i.c}$, 30 [W/m^{2}K] and radiation heat transfer coefficient, $h_{i.r} = 4\varepsilon\sigma T_r^3$, for $T_f = T_s = 400$ [°C] and $T_f = T_s = 600$ [°C] respectively.
- The heat transfer coefficient by convection on the unexposed side was assumed equal to
  a) 4 W/m^{2}K, according the to the EC1 recommendations (as default value)
  b) 10 W/m^{2}K, according the Ulf Wickström draft (Wickström, 2016) for the $T_g = 20$ [°C] and $T_s = 500$ [°C] (as alternative values)
- The emissivities of the steel surfaces were assumed equal to
  a) 0.9 both on exposed and the unexposed sides (as alternative values)
  b) 0.8 both on exposed and the unexposed sides (as default value)

Fire temperatures numerically calculated by using the new model have been compared with experimentally measured temperatures conducted in the compartment with non-insulated steel boundaries. Good agreement with the measured values and calculated temperatures were obtained as shown Figure 29.

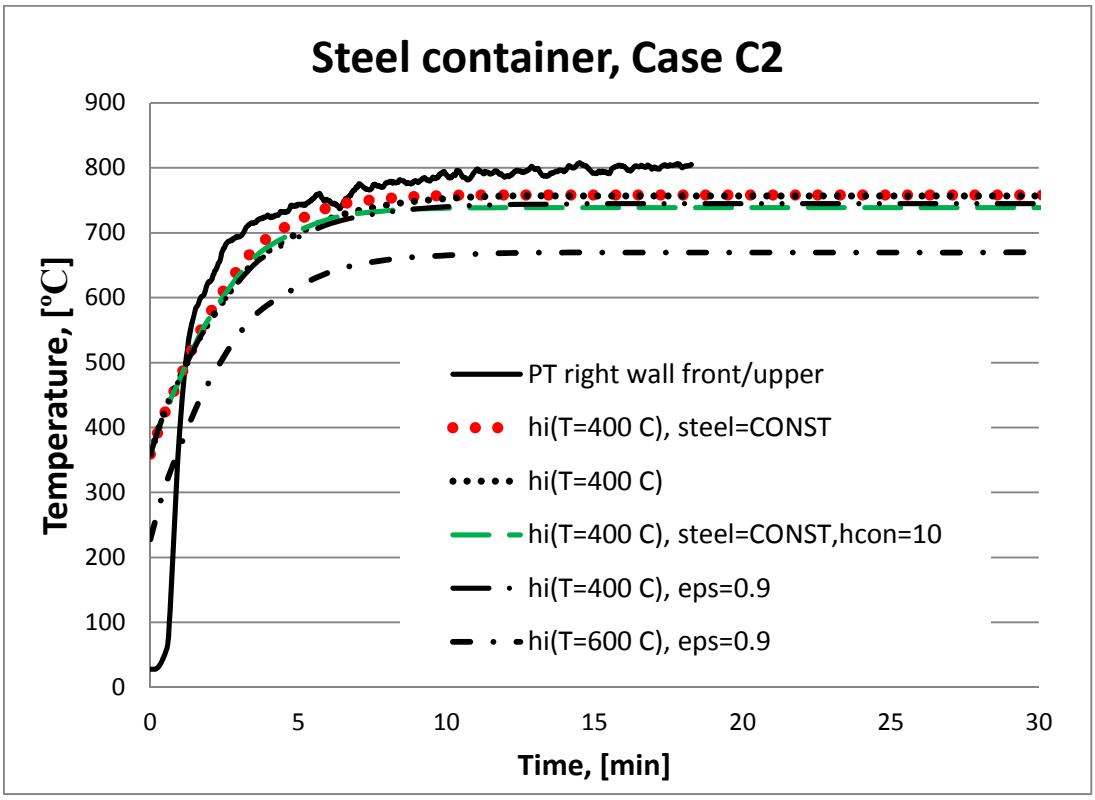

Figure 29. Comparison of calculated temperatures with measured higher temperature during experiments: Experimental measured temperatures with PT vs. calculated ones with Tasef. Non-insulated steel container.

As we can see on the Figure 29 the fire temperature during experiment goes above 800 °C, but the maximum steel temperature measured during experiments in the range of 500 to approximately 800°C, see Table 7, so the assumption of the heat transfer resistance between the fire gases and the exposed surface is kept at the constant values of $R_{i.tot} = 1/h_{i.tot}$ [m^{2}K/W], for $T_f = T_s = 600$ [°C] can be quite reasonable and have been used for analysis, see Figure 13.

Case D – steel structure insulated on the outside

The experiment with the highest HRR (1000kW) called D2 has been selected and compared.

Test series D was conducted on the same steel structure as test series C but with 50 mm of 200 kg/m^3 insulation boards on all external surfaces.

The stone wool had a nominal density of 200 kg/m^3 and a nominal room temperature conductivity of 0.04 W/mK, see Figure 10.

Assumptions:

- The heat transfer resistance between the fire gases and the exposed surface is kept constant:
  - $R_{h,i} = 1/h_i = 1/125$ [m^{2}K/W], for $T_f = T_s = 500$ [°C]

- $R_{h,i} = 1/h_i = 1/166$ [m^{2}K/W], for $T_f = T_s = 600$ [°C]
- $R_{h,i} = 1/h_i = 1/450$ [m^{2}K/W], for $T_f = T_s = 1000$ [°C]

(see Figure 24), where the convection heat transfer coefficient is assumed of h_{con}, 30 [W/m^{2}K] and radiation heat transfer coefficient, $h_{rad} = 4\varepsilon\sigma T_r^3$, for $T_f = T_s = 500$ [°C], $T_f = T_s = 600$ [°C] and $T_f = T_s = 1000$ [°C] respectively.

- The heat transfer coefficient by convection on the unexposed side was assumed equal to 4 W/m^{2}K, according the to the EC1 recommendations
- The emissivities of surfaces were assumed equal to 0.9 both on exposed and the unexposed sides.

Fire temperatures numerically calculated by using the new model have been compared with experimentally measured temperatures conducted in the compartment with insulated on the outside steel boundaries. Good agreement with the measured values and calculated temperatures were obtained as shown in Figure 30.

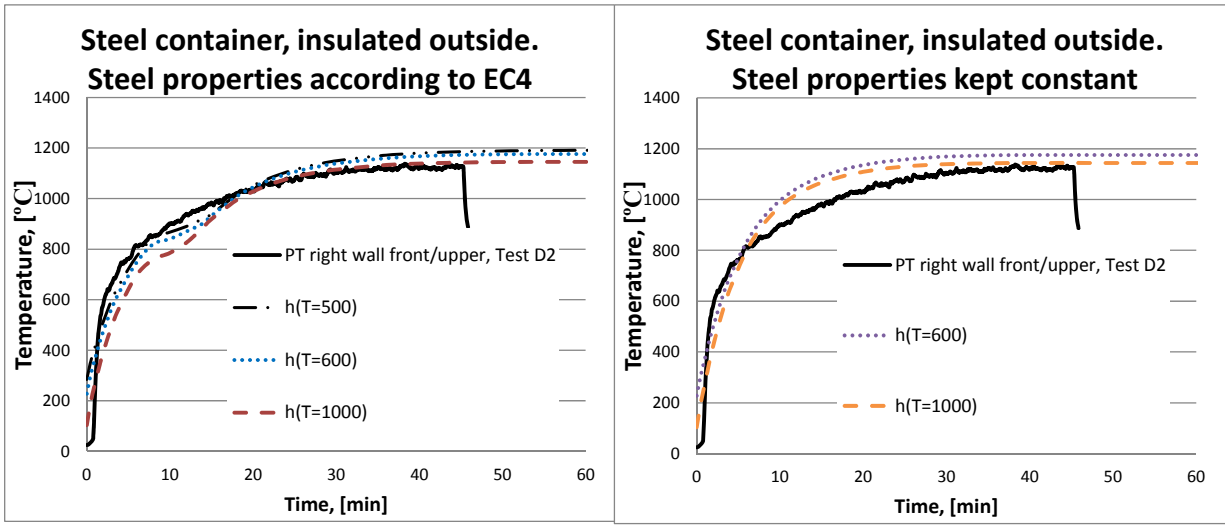

a) b)

Figure 30. Comparison of calculated temperatures with measured higher temperature during experiments: Experimental measured temperatures with PT vs. calculated ones with Tasef. Insulated ouside steel container.

LULEÅ TEKNISKA UNIVERSITET

Department of Civil, Enviromental and
Natural Resources Engineering
Luleå University oc Technology, SE
SE-971 87 Luleå, Sweden

http://www.ltu.se
Telephone: +46 920-49 10 00
Fax: +46 920-49 13 99

OUR SPONSORS & PARTNERS:

Brandforsk

SP your Science Partner

RAPPORTER UTGIVNA AV BRANDFORSK 2016:

2016:1 Utrymning i långa trappor uppåt: Utmattning, gånghastighet och beteende

2016:2 Förflyttning vid utrymning

2016:3 Dubbelglasfasader - En brandteknisk förstudie

2016:4 Utveckling och validering av enkla och praktiska modeller för beräkning av brandgastemperaturer i rum/brandceller

2016:5 Brandskyddsfärgens funktion vid riktiga bränder

2016:6 Detaljutformning av moderna betongkonstruktioner för att förbättra brandmotståndet

1979 bildades Brandforsk som svar på behovet av ett gemensamt organ för att initiera och finansiera forskning och utveckling inom brandsäkerhetsområdet.

Brandforsk är statens, försäkringsbranschens och industrins gemensamma organ för att initiera, bekosta och följa upp olika slag av brandforskning.

Huvudman för Brandforsk är Brandskyddsföreningen och verksamheten leds av en styrelse och bedrivs i form av projekt vid universitet och högskolor, forskningsinstitut, myndigheter och företag.

Brandforsk

Årstaängsvägen 21 c
Box 472 44, 100 74 Stockholm
Tel: 08-588 474 14
brandforsk@brandskyddsforeningen.se